

**Equation-of-motion technique for finite-size quantum-dot systems: Cluster expansion method**

Matthias Florian, Christopher Gies, and Frank Jahnke

*Institut für Theoretische Physik, University of Bremen, 28334 Bremen, Germany*

Heinrich A. M. Leymann and Jan Wiersig

*Institut für Theoretische Physik, Otto-von-Guericke-Universität Magdeburg, D-39016 Magdeburg, Germany*

(Received 15 October 2012; revised manuscript received 31 January 2013; published 25 April 2013)

An equation-of-motion based theory for the description of light emission from multilevel semiconductor quantum dots (QDs) is presented. It accounts for electronic excitations in the presence of Coulomb interaction, leading to multiexciton states, and their coupling to the quantized electromagnetic field. The two key aspects of this work concern (i) the combination of an exact treatment of the electronic degrees of freedom with an approximate approach for the photonic degrees of freedom that is based on the cluster expansion technique and (ii) the consistent incorporation of scattering and dephasing due to the coupling to delocalized electronic states and phonons into the equations of motion via Lindblad terms. Differences to previously used theories are discussed and results of the theory are shown for free-space emission, where multiexciton spectra are shown, and for emission into a single high- $Q$  cavity mode. In the latter case, a full solution of the von-Neumann equation is used to benchmark the proposed theory, which we term “finite-size hierarchy” (FSH) method.

DOI: [10.1103/PhysRevB.87.165306](https://doi.org/10.1103/PhysRevB.87.165306)

PACS number(s): 78.67.Hc, 78.20.Bh, 42.50.Pq, 85.60.—q

**I. INTRODUCTION**

Semiconductor heterostructures<sup>1</sup> are of central importance in the design of today’s optoelectronic devices with a wide application range in light emitters, detectors, and quantum information technology. Quantum dots (QDs) play an important role as active material in semiconductor lasers and quantum light emitters.<sup>2–8</sup> For the development of microscopic models, the cluster expansion technique<sup>9–20</sup> has been successfully used to address correlation effects due to various many-body interactions. In semiconductors, many-body effects are present due to carrier-photon and carrier-carrier Coulomb interactions as well as the interaction between carriers and phonons. The idea of the cluster expansion technique is to formulate equations of motion for correlation functions up to a given order  $N$  and to express all expectation values of interest in terms of these correlation functions. The underlying assumption is the presence of a large Hilbert space for the many-body excitations, so that the configuration averages render higher-order correlations increasingly unimportant. The cluster expansion technique has initially been applied to systems with many degrees of freedom, where the number of possible electronic configurations by far exceeds the highest number of considered  $N$ -particle correlations (typically  $N = 2, 3, 4$ ). This included, for example, photoluminescence,<sup>21</sup> resonance fluorescence,<sup>11</sup> exciton formation dynamics<sup>12</sup> in quantum-well systems, quantum dynamics of condensed Bose gases,<sup>22</sup> and spin dynamics of ferromagnetic system.<sup>23</sup>

More recently, applications have been extended to QD-based systems, where the cluster expansion method has successfully been used to study quantum-optical and related effects, like photon anti-bunching and coherence properties of the light emission,<sup>13,19,24,25</sup> coherent emission of cavity phonons,<sup>26</sup> correlation build-up,<sup>27</sup> quantum spectroscopy,<sup>28</sup> as well as the influence of Coulomb-induced carrier correlations.<sup>14–16</sup> In QDs, the carrier confinement results in a small number of localized states, which contrasts the situation in quasicontinuous systems like quantum wells.

In both theory and experiment,<sup>29</sup> QDs with only a few or even a single localized electron state have been considered. It is one aim of this paper to discuss the implications of the system-size limitation to the application of the cluster expansion and to propose a new way to describe systems in which the small size of the electronic Hilbert space leads to strongly enhanced correlations.

The single-QD case is often addressed with methods from atomic quantum optics, where the emitter is represented by a few-level system. The nonperturbative interaction with a high- $Q$  cavity mode via the Jaynes-Cummings Hamiltonian and the perturbative interaction with a continuum of free-space modes via Lindblad terms can be treated by directly solving the von-Neumann equation for the density matrix of the electronic system and the cavity mode.<sup>30</sup> This requires the underlying Hilbert space to be small enough and is currently only feasible for a single or very few emitters. Examples for applications to single-QD systems are.<sup>31,32</sup> Recently, the authors have presented a QD theory in which the von-Neumann dynamics includes both the Jaynes-Cummings and the Coulomb Hamiltonians, accounting for the interplay of various multiexciton configurations and the nonperturbative treatment of the light-matter interaction.<sup>33,34</sup> Furthermore, based on the von Neumann dynamics including the Coulomb Hamiltonian, the influence of multiexciton effects on the efficiency of carrier scattering has been studied.<sup>35</sup> When considering explicitly the case of many individual emitters or the emission into many modes, however, the size of the Hilbert space precludes direct calculations of the many-particle density matrix, and one has to retreat to approximate many-body methods like the cluster expansion technique.

Another central point addressed in this paper is the consistent description of scattering and dephasing in the equation-of-motion approach. QDs are embedded systems and coupled to continuum states of the surrounding material. The Coulomb interaction and the coupling to LO-phonons leads to efficient carrier scattering processes between localized and delocalized states, feeding carriers into the QD after

off-resonant excitation into the continuum states of the barrier material, as well as being a source of dephasing. A Hamiltonian description of these scattering processes is naturally possible within an equation-of-motion approach, but practically challenging.<sup>12,25</sup> More often, scattering and dephasing were accounted for phenomenologically by adding constant rates to the equations of motion. Especially for equations describing the dynamics of higher-order correlation functions, this may lead to inconsistencies and produce artifacts, such as heating.<sup>12</sup> In quantum optics, one typically discriminates between the system and environmental degrees of freedom and treats the interaction of the system with the environment via Lindblad terms<sup>36</sup> that are added to the von-Neumann equation. As we show, this can be carried over to an equation-of-motion based approach, because the carrier dynamics in QDs naturally separates into the system, represented by the localized states, and the environment, provided by the quasicontinuum of delocalized states. Then the Coulomb and light-matter interactions are fully accounted for the localized QD states, while the interaction processes with the continuum states are described via Lindblad terms. These can be obtained with standard many-body techniques.<sup>35,37–39</sup> The result is a consistent formulation of scattering and dephasing that is free of the problems associated with the phenomenological approaches.

We begin by addressing the equation-of-motion technique for the carrier system, before we introduce and classify mixed-operator correlation functions that are subject to different interactions. The “finite-size hierarchy” (FSH) method is introduced in which we combine an exact treatment of the carrier degrees of freedom with an approximate cluster expansion approach for the arising hierarchy in the photon operators. In Sec. III, we specify the nature of the environment coupling and the inclusion in the theoretical formalism. In order to apply the theoretical framework in the following sections, a specific QD system is introduced in Sec. IV. We derive equations of motion for the Hamiltonian time evolution of the QD carriers as well as the dissipative interaction with carriers in delocalized states. Section V is devoted to emission into a continuum of free-space modes. Here, we discuss how carrier correlations give rise to multiexcitonic effects in the emission spectra and how the various scattering and dephasing processes manifest themselves in the line widths of the various emission peaks. A comparison with the conventional cluster expansion technique reveals insight into the physical representation of the system by a limited number of correlation functions. Numerical results for the emission of a single QD in a microcavity are presented in Sec. VI. For this system, we are able to compare the approximate treatment of the system dynamics in terms of the cluster expansion method to an exact solution obtained from the FSH and von-Neumann equation. This comparison illustrates the impact of the truncation at different orders in the hierarchy of photon operators and demonstrate the applicability of the FSH method. Finally, in Sec. VII two different incoherent excitation mechanisms are discussed.

## II. MANY-BODY TREATMENT OF THE EMBEDDED QD SYSTEM

QDs are embedded systems and their electronic single-particle states are coupled to those of the surrounding

environment by the Coulomb interaction and the interaction with LO phonons. It is important to stress that correlations amongst QD carriers are dominated by the interaction within the dot as well as, e.g., in the presence of a resonator, by the interaction with photons. Based on this, we treat the localized electronic degrees of freedom explicitly, fully accounting for the Coulomb interaction amongst QD carriers and their light-matter interaction. In this section, we focus on the system dynamics and its formulation in the von-Neumann and equation-of-motion approaches. The coupling of the environment states to the system dynamics via Lindblad terms is discussed in Sec. III.

The system dynamics is determined by the von-Neumann equation

$$\frac{d}{dt} \rho = -i[\mathcal{H}, \rho]. \quad (1)$$

Here, we consider the free electronic contributions to the Hamiltonian  $\mathcal{H}$  as well as the Coulomb interaction and subsequently in Sec. II B also the Jaynes-Cummings interaction. The time-dependent solution of Eq. (1) then includes the full configuration interaction (FCI) due to the Coulomb Hamiltonian. The electronic Hilbert space is finite and limited by the possible number of carriers that the QD system can accommodate. In (quasi-) continuous systems this limitation is merely formal. In a QD with only few confined states, however, the limitation is perceivable and may even allow for a direct solution of Eq. (1), see, e.g., the Refs. 31 and 32 for a small and Refs. 34 and 40 for a large number of configurations.

By suitable tracing of the many-body density matrix, Eq. (1) can be rewritten into a hierarchy of equations of motion for expectation values, in which single-particle expectation values are coupled to two-particle expectation values, and so on. The hierarchy of coupled equations is limited by the finite size of the Hilbert space that introduces a natural truncation. This can also be understood by considering the fact that only those normal-ordered operator averages, addressing up to the maximum possible number of carriers in the system, can be different from zero, as the consecutive application of a number of creation or annihilation operators that exceeds the number of possible single-particle states must give a vanishing contribution. As long as no further approximations are introduced, both the density-matrix and the equation-of-motion approaches are equivalent. For a system with mixed hierarchies in carrier and photon operators, this equivalence will be used to establish the link between the “exact” von-Neumann-based treatment for the electronic degrees of freedom for which we introduce the name “finite-size hierarchy” (FSH) method and the approximate cluster expansion method in which the electronic hierarchy is truncated typically at an order that is lower than the size limitation of the Hilbert space.

### A. Equation-of-motion formulation for the electronic degrees of freedom

We begin by schematically formulating the hierarchy of equations of motion for a system that can accommodate up to  $N_{\max}^{c,v}$  conduction- and valence-band carriers per spin direction. Since the successive application of  $N_{\max}^c + 1$  conduction-band electron or  $N_{\max}^v + 1$  valence-band electron annihilation

operators yields zero, an automatic truncation of the hierarchy is implied. To achieve a simplification of the following discussion, we consider from here on equal numbers of confined states in both bands, so that the highest operator average that can differ from zero contains  $2(N_{\max}^c + N_{\max}^v) \equiv 4N_{\max}$  carrier operators.

In the following, we embrace the formulation of the cluster expansion where correlation functions are used instead of operator averages. As long as the hierarchy of equations is not terminated at an order below its natural truncation, both formulations are equivalent. However, if a truncation is desired, a formulation in terms of correlation functions is better suited. A correlation function of the order  $N$  is defined as

$$\delta\langle N \rangle = \langle N \rangle - \delta\langle N \rangle_F, \quad (2)$$

where  $\delta\langle N \rangle_F$  represents products of all possible factorizations of the operator expectation value  $\langle N \rangle$  into correlation functions of orders smaller than  $N$ . (In case of fermionic operators, a sign change is required if an odd number of permutations is necessary to regain normal ordering.) The order  $N$  is defined as half the number of carrier operators. For example, occupation probabilities of single-particle states  $\langle c_i^\dagger c_i \rangle$  and  $\langle v_i^\dagger v_i \rangle$  (for the notation see Appendix A) are of first order (singlets) that represent uncorrelated entities,

$$\delta\langle 1 \rangle \equiv \langle 1 \rangle. \quad (3)$$

Examples for correlation functions of the order  $N = 2$  (doublets) are  $\delta\langle c_i^\dagger c_j^\dagger c_k c_l \rangle$  or  $\delta\langle v_i^\dagger v_j^\dagger c_k v_l \rangle$ .

The hierarchy defined by Eqs. (2) and (3) terminates due to the discussed limitation in operator averages to  $2N_{\max}$  carrier operators and is represented by the *boundary condition*

$$\delta\langle N \rangle = -\delta\langle N \rangle_F \quad \text{if } N > N_{\max}. \quad (4)$$

For  $N = N_{\max} + 1$ , Eq. (4) terminates the coupling to higher expectation value and ensures a correct treatment of the finite carrier system, so that indeed the formulation in terms of dynamical equations for correlation functions is equivalent to a solution of Eq. (1) for the corresponding finite set of basis states.

When the electronic Hilbert space, and correspondingly the number of electronic degrees of freedom is large, an inclusion of correlation functions up to this level is neither possible nor necessary. This defines the regime of applicability of the cluster expansion method, where suitable approximations are based on a truncation of the hierarchy at a level much lower than  $N_{\max}$ , realized by setting all correlation functions above a certain cutoff  $N_{\text{trunc}}$  to zero:

$$\delta\langle N \rangle = 0 \quad \text{if } N > N_{\text{trunc}}. \quad (5)$$

In what comes next, it is important to emphasize that this procedure introduces two separate approximations. Firstly, the influences of correlated processes involving more than  $N_{\text{trunc}}$  carriers are neglected. Secondly, for  $N > N_{\max}$  there is a contradiction between Eqs. (4) and (5) in the sense that the latter formally violates the boundary condition due to the finite system size. We discuss the implications of both approximations in the following.

For an approximate treatment of carrier correlations in large systems, the order up to which  $N$ -particle correlations need to

be calculated depends on the strength of dephasing processes on the one hand, and on the quantities of interest on the other. Scattering processes, introduced, e.g., by the Coulomb- and LO-phonon interactions, are responsible for damping out correlation effects, and so are cavity losses that act on the photonic subsystem, see Sec. II B. Higher-order correlation functions are typically subject to stronger dephasing, so that their impact on the dynamics of lower-order quantities decreases with increasing  $N$ . Nevertheless, if correlation effects themselves are of interest, the corresponding correlation functions must be accounted for, and corrections due to the next higher order may be relevant even if the impact on lower orders is small. For example, exciton formation is described by second-order correlation functions  $\delta\langle c_i^\dagger v_j^\dagger c_k v_l \rangle$ . Their study therefore requires going beyond the singlet level.

The error introduced by the violation of the boundary condition (4) depends on the system size in relation to the order  $N_{\text{trunc}}$  at which the cutoff is performed as well as on the strength of dephasing processes in the system that assist in damping out correlations. In large systems, where the allowed number of carriers exceeds the cutoff by orders of magnitude, the effect of violating the boundary condition at the highest order is imperceptible. In QDs with only few localized states, the situation may be entirely different, and this is the point we are addressing. If the cutoff  $N_{\text{trunc}}$  imposed by an approximative treatment is close to the intrinsic cutoff  $N_{\max}$ , the error made in replacing Eq. (4) by Eq. (5) is more likely to propagate into those correlation functions that are kept and become significant. In terms of the underlying physics, the restriction to a few-particle system enhances higher-order carrier correlations. In Sec. IV, we will focus on a particular QD with two confined states for electrons and holes and show that the cluster expansion method is, in fact, not applicable to the electronic subsystem, and the exact description including Eq. (4) must be used instead.

## B. Many-body description for mixed expectation values

We now turn to the case that a hierarchy arises not only in the electronic degrees of freedom, but also due to other interactions that may explicitly appear in the Hamiltonian, like the coupling to photons or phonons. Extra thought must be given how to classify the order and how to perform the truncation of the arising hierarchies of mixed-operator expectation values.

As an example, consider the time derivative of a conduction band carrier and a photon annihilation operator with respect to the light-matter interaction Hamiltonian  $\mathcal{H}_{\text{LM}}$  (see Appendix A):

$$\left. \frac{d}{dt} c_i \right|_{\mathcal{H}_{\text{LM}}} = - \sum_{\xi} g_{\xi} b_{\xi} v_i, \quad (6a)$$

$$\left. \frac{d}{dt} b_{\xi} \right|_{\mathcal{H}_{\text{LM}}} = \sum_i g_{\xi}^* v_i^{\dagger} c_i. \quad (6b)$$

Two hierarchies are introduced, one in the photon operators and one in the carrier operators: In the equation of motion for a carrier operator (6a), an additional photon operator is added, and vice versa, a carrier transition  $v_i^{\dagger} c_i$  is associated with the derivative of a photon operator in Eq. (6b).

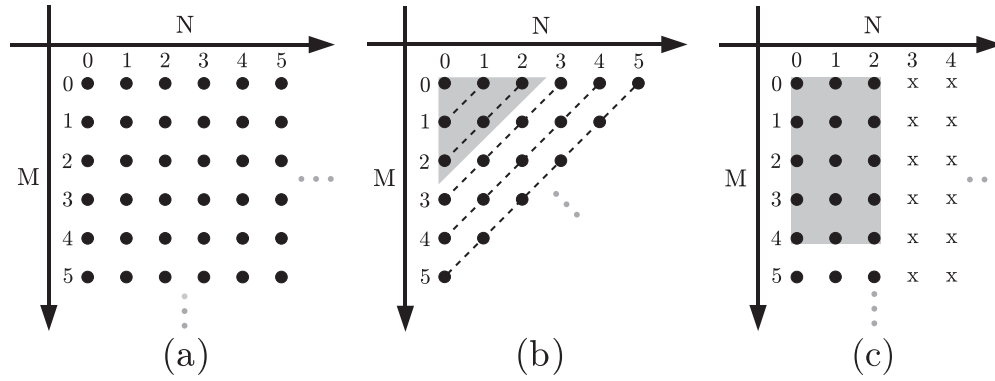


FIG. 1. (a) Illustration of the classification of mixed correlation functions  $\delta\langle N, M \rangle$  according to the number of carrier ( $2N$ ) and photon ( $M$ ) operators (represented by dots). (b) Classification and truncation employed by the conventional cluster expansion method. Mixed correlation functions are treated by a single hierarchy of order  $N + M$ . The shaded area encloses those correlations up to the doublet level  $(N + M)_{\text{trunc}} = 2$ . (c) A situation found in a system where the number of electrons and holes is limited to two. Then the hierarchy of carrier operators closes naturally on the four-operator level  $N_{\text{max}} = 2$  and is, in principle, not restricted in the number of photon operators  $M$ . A truncation must be performed manually. As an example, the shaded area shows the necessary correlation functions for  $M_{\text{trunc}} = 4$ .

Regarding the additional light-matter interaction, we introduce a classification of mixed correlation functions  $\delta\langle M, N \rangle$ , containing  $M$  photon and  $2N$  carrier operators by the tuple of numbers  $(M, N)$ . Equation (2) is generalized to

$$\delta\langle M, N \rangle = \langle M, N \rangle - \delta\langle M, N \rangle_F, \quad (7)$$

where the factorization  $\delta\langle M, N \rangle_F$  contains all possible products of lower-order correlation functions of order  $(M', N')$  that meet the three criteria  $N' \leq N$ ,  $M' \leq M$ , and  $N' + M' < N + M$ . The classification is illustrated in Fig. 1(a), where each set of correlation functions of the order  $(M, N)$  is represented as a dot.

This suggested classification scheme serves two purposes; on the one hand, it offers a clear-cut definition of the correlation effects included at each order, namely, those involving  $N$  carriers and  $M$  photons. On the other hand, it provides a platform to treat the two hierarchies in a different fashion, which we discuss in detail below.

A different classification scheme has been used in the past and is typically associated with the cluster expansion method.<sup>11,18</sup> There, mixed correlation functions  $\delta\langle M, N \rangle$  are classified by a single number  $M + N$ , as schematically depicted in Fig. 1(b). It is based on the observation that the coupling of carriers and photons, provided by the Jaynes-Cummings Hamiltonian, leads to the formal equivalence of a photon annihilation operator and an electron-hole-pair creation operator. Correlation functions with  $N + M = 1, 2, 3, 4, \dots$  have been termed singlets, doublets, triplets, quadruplets, and so on. As described for the electronic system in Sec. II A, a cutoff  $(N + M)_{\text{trunc}}$  is performed, and all higher-order correlation functions are approximated as zero in the fashion of Eq. (5),

$$\delta\langle M, N \rangle = 0 \quad \text{if} \quad N + M > (N + M)_{\text{trunc}}. \quad (8)$$

An illustration is given in Fig. 1(b), where the shaded area corresponds to those correlation functions kept up to the doublet level. The cluster expansion method based on this scheme has been used for systems where the truncation was performed at an order much lower than the implicitly assumed

size of the electronic subsystem (the photonic subsystem is, by nature, not limited).<sup>11,12</sup>

This brings us to the question how to formulate the hierarchy problem in systems where the electronic subsystem is limited to accommodate a small number of carriers, which leads to the definition of the *finite-size hierarchy (FSH) method*. As we have discussed for the electronic subsystem in the absence of additional interactions in Sec. II A, the approximate treatment of the cluster expansion method introduces errors in the boundary condition that may require an exact treatment of the electronic degrees of freedom in a fashion analog to the von Neumann equation. For a system with mixed-operator correlation functions  $\delta\langle M, N \rangle$ , the boundary condition (4) can be generalized to

$$\delta\langle M, N \rangle = -\delta\langle M, N \rangle_F \quad \text{if} \quad N > N_{\text{max}}. \quad (9)$$

The exact treatment of electronic correlations requires taking all correlation functions  $\delta\langle M, N \rangle$  up to  $N = N_{\text{max}}$  into account and to satisfy Eq. (9) at the highest level  $N = N_{\text{max}}$ . The photonic hierarchy is not limited and must be truncated at a manually introduced cutoff  $M_{\text{trunc}}$ . The order at which this approximation is performed depends on the quantities of interest as well as on the relationship between correlation built-up and dephasing. A schematic illustration is found in Fig. 1(c), where the number of electrons and holes is restricted to  $N_{\text{max}} = 2$ , and the truncation is performed at  $M_{\text{trunc}} = 4$  photons.

Summarizing this section, starting from the general form of the von-Neumann equation, the treatment of an electronic system residing in a finite Hilbert space can be formulated as a closed set of equations of motion for correlation functions, fully representing the electronic degrees of freedom (FSH method). An additional hierarchy in the photon operators spoils the exact representation, as all electronic operator averages can appear with additional photon operators. The hierarchy in terms of photon operators requires an approximate truncation in the fashion of the cluster expansion method. This is, however, uncritical and works very well in practice, as we will demonstrate in Sec. VI.

Performing an additional truncation also on the electronic degrees of freedom constitutes a different approximation that is much more intricate. A discussion of the manifestation of differences between the cluster expansion and FSH methods is found in Secs. V and VI.

### III. ENVIRONMENT COUPLING: TREATMENT OF SCATTERING AND DEPHASING PROCESSES

The localized states of self-assembled QDs are generally coupled to delocalized states of the surrounding semiconductor matrix material. In experiments and device applications, carriers are excited optically or electrically in these continuum states. The successive capture into the localized QDs states is mediated by scattering processes with carriers in the continuum, but also with lattice vibrations that are known to effectively exchange excess energy by emission/absorption of phonons.<sup>41–44</sup> Redistribution by scattering of carriers is always accompanied by dephasing. Dephasing of coherences and correlations in QD-based nanostructures is of central importance for the emission properties of devices.

The discrete nature of the localized states in QDs allows for the possibility to make a distinction between the QD system and its environment, where the dynamics of the first is fully accounted for by contributions to the system Hamiltonian, and the latter are treated in a system-bath approach. The purpose of Sec. III A is the specification of both components and the description of the Lindblad formalism that is commonly used to model system-reservoir coupling within the von-Neumann equation. This is carried over to the equation-of-motion approach for expectation values in Sec. III B to provide a consistent platform to include scattering and dephasing contributions. The consistent inclusion of dephasing is a major advancement from previous versions of the theory and one of the central achievements in this work.

#### A. System-reservoir interaction

In quantum well or bulk material, a large number of carriers are distributed amongst dense-lying states that are generally treated as a continuum. Processes involving the continuum states, such as carrier-carrier scattering, optical recombination, and scattering with phonons, must be treated on equal footing. In QDs the situation is different. The three-dimensional carrier confinement leads to a discretization of the single-particle density of states. Typical self-assembled QDs are grown on a wetting layer (WL) and the whole system is embedded in a barrier material. The energy of the lowest-lying continuum states of the WL provides an energetic upper bound for the localized QD states and, therefore, limits their number.

One, therefore, finds the situation in which the localized states are responsible for the recombination dynamics of interest, whereas the nearby continuum provides carriers that can be captured into the localized states or serve as scattering partners for carriers in the QD states. A separation into system, consisting of the localized states, and reservoir, consisting of the continuum states, is justified if the interaction between the two does not lead to a mixing of states (hybridization). The dynamics of carriers in the continuum states is determined by an excitation process, by scattering amongst carriers in

the continuum as well as by the interaction with carriers in the localized QD states. The first two effects can be accommodated in the calculation of the rates  $\gamma_\eta$ . The last effect only plays a role if the QD recombination dynamics has a noticeable impact on the continuum dynamics, as it would be the case in a microcavity laser with many QDs.

The contribution of the reservoir, which can either be seen as a fermionic or a bosonic bath (depending if a coupling to carriers in the continuum, or to phonons is considered), to the density operator can be treated, e.g., in the Born-Markov approximation. This approach leads to a Lindblad term  $\mathcal{L}_\eta$ <sup>36,45</sup> for *each* capture and relaxation process (in the following, denoted by the index  $\eta$ ) associated with the considered reservoir and of the form

$$\frac{d}{dt} \rho \Big|_{\mathcal{L}_\eta} = \frac{\gamma_\eta}{2} \left[ \sum_{\alpha, \beta} 2 |f_\alpha^\eta\rangle \langle i_\alpha^\eta| \rho |i_\beta^\eta\rangle \langle f_\beta^\eta| - \sum_\alpha (|i_\alpha^\eta\rangle \langle i_\alpha^\eta| \rho - \rho |i_\alpha^\eta\rangle \langle i_\alpha^\eta|) \right]. \quad (10)$$

Here,  $\gamma_\eta$  is referred to as the corresponding capture/relaxation rate and  $|i_\alpha^\eta\rangle$  are the initial and  $|f_\alpha^\eta\rangle$  the final configurations of the described scattering process. The contribution of the Lindblad terms to the dynamical equations for the diagonal elements of the density matrix  $\rho$ ,

$$\frac{d}{dt} \langle f_\alpha^\eta | \rho | f_\alpha^\eta \rangle = \gamma_\eta \langle i_\alpha^\eta | \rho | i_\alpha^\eta \rangle = -\frac{d}{dt} \langle i_\alpha^\eta | \rho | i_\alpha^\eta \rangle, \quad (11)$$

reflect the trace-conserving nature of the Lindblad form, leading to an equilibration of the system with respect to the bath at a characteristic time  $1/\gamma_\eta$ , determined by the QD level-spacing, the lattice temperature, and the carrier density. Additionally, dephasing originates from the contribution of the second line in Eq. (10) to the equations for the nondiagonal elements of the density matrix, i.e.,

$$\frac{d}{dt} \langle i_\alpha^\eta | \rho | f_\alpha^\eta \rangle = -\frac{\gamma_\eta}{2} \langle i_\alpha^\eta | \rho | f_\alpha^\eta \rangle, \quad (12)$$

and its complex conjugate. Thus all optical transitions involving  $|i_\alpha^\eta\rangle$  and/or  $|f_\alpha^\eta\rangle$  as an initial/final state are consistently dephased by the process  $\eta$ .<sup>34,40</sup> More sophisticated many-body methods beyond the Born-Markov limit,<sup>35,46,47</sup> as well as experimental results,<sup>29,48</sup> can be used to determine more accurate rates  $\gamma_\eta$ , which enter this formalism as input parameters.

#### B. Lindblad terms in the equation-of-motion technique

The time evolution of the density operator is determined by the von-Neumann equation with the Hamiltonian part  $\mathcal{H}$  and the dissipative Lindblad-type superoperator  $\mathcal{L}_\eta$  according to Eq. (10), which can be written as

$$\frac{d}{dt} \rho = -i[\mathcal{H}, \rho] + \sum_\eta \mathcal{L}_\eta \rho. \quad (13)$$

This we refer to as the von-Neumann-Lindblad (vNL) equation. Once the solution is known, arbitrary single-time operator averages  $\langle \mathcal{O} \rangle$  can be obtained by taking the trace  $\text{Tr} \{ \rho \mathcal{O} \}$ .

Equations of motion are derived by considering the time evolution of expectation values  $\langle A \rangle = \text{Tr} \{ \rho A \}$ , expressed by Heisenberg's equation of motion for operator averages for

which the explicit knowledge of  $\rho$  is not required, see Sec. II. A natural way to include the Lindblad contributions in the many-body formalism is to add them to the equations of motion, which follows directly from the von-Neumann-Lindblad equation (13) by calculating operator averages and leads to

$$\frac{d}{dt} \langle A \rangle = i \langle [\mathcal{H}, A] \rangle + \sum_{\eta} \frac{\gamma_{\eta}}{2} (\langle [\sigma_{\eta}^{\dagger}, A] \sigma_{\eta} \rangle + \langle \sigma_{\eta}^{\dagger} [A, \sigma_{\eta}] \rangle) \quad (14)$$

with  $\sigma_{\eta} = \sum_{\alpha} |f_{\alpha}^{\eta}\rangle \langle i_{\alpha}^{\eta}|$ .

Both the interaction parts of the Hamiltonian and the Lindblad contributions in the above equation introduce a hierarchy of coupled equations. What has been discussed for the Hamiltonian contributions in Sec. II also applies for the latter with respect to finite system size and truncation.

The proposed method has the benefit of a consistent inclusion of scattering and dephasing in a reservoir fashion, while rates for the interaction with the carrier and phonon reservoirs can be obtained from separate calculations of desired sophistication. In the past, dephasing has often been included phenomenologically by adding a constant dephasing rate  $\Gamma$  to the dynamical equations for expectation values associated with polarizations.<sup>14,15,24,49</sup> Next to providing dephasing, this method has been shown to introduce artifacts, like artificial heating of the system.<sup>12</sup> A consistent formulation of dephasing requires a relationship between both, that is expressed in Eqs. (11) and (12).

#### IV. EQUATIONS OF MOTION

In the following, we will illustrate the FSH method by deriving the dynamical equations for a particular QD-microcavity system. So far, the model has been formulated for an arbitrary type and number of single-particle states. However, it greatly simplifies our discussion and the resulting equations if we consider a QD with only two confined states for electrons and holes each. These levels we refer to as  $s$  and  $p$  shells. Furthermore, only carriers of one spin direction are considered. The restriction to one spin subsystem has been shown<sup>34,40</sup> to constitute a reasonable approximation in the regime of strong off-resonant excitation in self-assembled QDs, where scattering processes with quasicontinuum carriers broaden the spectral lines. For applications like low-excitation spectroscopy, the QD system must be augmented to explicitly contain the spin degree of freedom. On the two-particle-correlation level this situation has, e.g., been studied by Hohenester *et al.*<sup>51</sup>

In Secs. IV–VI, we will use an additional approximation that considerably simplifies the arising hierarchy of equations and that we would like to discuss in detail. The total number of possible configurations in the described QD is 16, since zero to four electrons can be distributed amongst four localized single-particle states. The FSH method, in which the electronic degrees of freedom are treated exactly, requires to take operator averages with up to  $2(N_{\max}^c + N_{\max}^v) = 8$  carrier operators into account. The highest possible-carrier operator average that can differ from zero is the four-particle quantity

$$\langle c_s^{\dagger} c_p^{\dagger} v_s^{\dagger} v_p^{\dagger} v_p v_s c_p c_s \rangle. \quad (15)$$

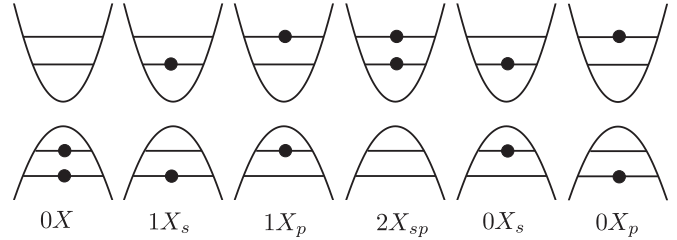


FIG. 2. Possible configurations in a four-level QD, in which valence- and conduction-band carriers are excited and de-excited only in pairs. The representation is given in the conduction-valence-band (cv) picture.

A derivation of the equations of motion for the corresponding correlation functions is a cumbersome and error-prone endeavor and only recommended with an automatic generation algorithm. For this work, a separate program has been written in FORM<sup>52</sup> to fulfill this goal. For simplification purposes, we restrict the number of possible configurations by the following assumptions. (1) An effective pair-wise carrier capture in which the in-scattering of an electron into the QD  $p$  shell is always accompanied by the in-scattering of a hole (in the cv picture: a carrier present in the valence-band  $p$  state is excited into the conduction-band  $p$  state). (2) Only intraband scattering processes preserving the carrier number within the QD are considered.

Since, in the cv picture, the optical recombination is also carrier-number conserving, only the six configurations shown in Fig. 2 can form under this condition, all of which contain two carriers in the system. Thus the largest operator averages that have to be evaluated for a system with the boundary condition  $N_{\max}^c = N_{\max}^v = 2$  are those with up to four carrier operators, plus additional photon operators. One example is discussed in the beginning of Sec. V in the context of biexcitonic recombination.

Several scattering processes are accounted for: the discussed pair-wise capture of carriers from the continuum into the localized  $p$  states at rate  $P$ , as well as scattering from the conduction band  $p$  to  $s$  shell and valence-band  $s$  to  $p$  shell via the rates  $\gamma_{sp}^{cc}$  and  $\gamma_{ps}^{vv}$ . The rates  $\gamma_{ps}^{cc}$  and  $\gamma_{sp}^{vv}$  correspond to the reverse processes. The model system together with the considered scattering and recombination processes is sketched in Fig. 3.

This section is split into two parts in which the FSH hierarchy is derived: the first Sec. IV A deals with the dynamics due to the Hamiltonian contributions using the light-matter interaction as an example. Contributions due to other parts of the Hamiltonian are given in Appendix B. In Sec. IV B, contributions from the system-reservoir interaction are discussed. A special emphasis is placed on the differences between the FSH and the cluster expansion method and deviations occurring in the equations are pointed out.

##### A. Hamiltonian dynamics

The lowest-order observables of interest are the carrier populations as well as the mean number of cavity photons. Higher-order operator averages appear in the derivation of equations of motion. The arising hierarchy is finite in the

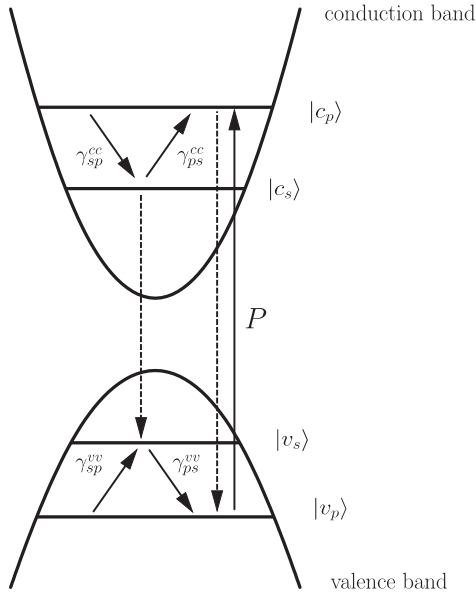


FIG. 3. QD model with the considered rates  $\gamma$  for electrons in the conduction and valence bands, describing scattering into and out of the  $s$  shell. Carrier generation is modeled by a transition process between the  $p$  levels at rate  $P$ . Light-matter coupling leads to recombination processes between the  $s$  and the  $p$  states due to spontaneous emission (dashed arrows).

carrier degrees of freedom, while the photonic hierarchy is truncated at the  $M_{\text{trunc}} = 2$  level, see Sec. II B.

The contribution of the light-matter interaction  $\mathcal{H}_{\text{LM}}$  to Heisenberg's equations of motion for the conduction band carrier population  $f_i^c = \langle c_i^\dagger c_i \rangle$ , are given by

$$\left. \frac{d}{dt} f_i^c \right|_{\mathcal{H}_{\text{LM}}} = -2 \text{Re} \sum_{\xi} g_{\xi}^* \Pi_{\xi,i}. \quad (16)$$

The real part of the photon-assisted polarization  $\Pi_{\xi,i} = \delta \langle b_{\xi}^{\dagger} v_i^{\dagger} c_i \rangle$  describes transition amplitudes between QD levels, and is proportional to the light-matter coupling strength  $g_{\xi}$ . In order to solve Eq. (16) additional dynamical equations for the photon-assisted polarization, which are one step up in the hierarchy with respect to photon operators, are required and evolve as

$$\begin{aligned} \left. \frac{d}{dt} \Pi_{\xi,i} \right|_{\mathcal{H}_{\text{LM}}} &= g_{\xi} f_i^c (1 - f_i^v) + g_{\xi} \sum_{\alpha} C_{\alpha i i \alpha}^x \\ &+ g_{\xi} \mathcal{N}_{\xi} (f_i^c - f_i^v) + g_{\xi} \mathcal{N}_{\xi,i}^c - g_{\xi} \mathcal{N}_{\xi,i}^v. \end{aligned} \quad (17)$$

The recombination of a QD excitation described by  $\Pi_{\xi,i}$  does not only require the presence of a conduction-band carrier, but also the nonoccupancy of a valence-band state, which ends up in an emission rate proportional to  $\langle c_i^{\dagger} v_i v_j^{\dagger} c_j \rangle$  (see Ref. 11). In Eq. (17) enters the decomposition of this expectation value in a contribution of two uncorrelated carriers  $\propto f_i^c (1 - f_i^v)$  in the upper and lower states, plus interband carrier correlations  $\propto C_{ijji}^x := \delta \langle c_i^{\dagger} v_j^{\dagger} c_j v_i \rangle$  according to Eq. (2). Thus the first line in Eq. (17) can be identified as the source term of spontaneous emission, naturally appearing within this formalism due to quantization of the light field. The second line of Eq. (17) arises from mixed expectation values  $\langle b_{\xi}^{\dagger} b_{\xi} c_i^{\dagger} c_i \rangle$  and  $\langle b_{\xi}^{\dagger} b_{\xi} v_i^{\dagger} v_i \rangle$  of

which the uncorrelated contribution is proportional to the photon number  $\mathcal{N}_{\xi} := \langle b_{\xi}^{\dagger} b_{\xi} \rangle$  and can be attributed to stimulated emission and absorption, whereas  $\mathcal{N}_{\xi,i}^c := \delta \langle b_{\xi}^{\dagger} b_{\xi} c_i^{\dagger} c_i \rangle$  and  $\mathcal{N}_{\xi,i}^v := \delta \langle b_{\xi}^{\dagger} b_{\xi} v_i^{\dagger} v_i \rangle$  represent carrier-photon correlations. Note that  $\langle b_{\xi}^{\dagger} \rangle$  and  $\langle v_i^{\dagger} c_j \rangle$  vanish in the incoherent regime. Throughout this paper, we do not account for correlations between different optical modes. This is well justified in the presence of a microresonator, where a single cavity mode strongly dominates over all other leaky and detuned cavity modes. When free space emission is considered, mode coupling effects may play a role and an evaluation of such terms can be considered. One must be aware, however, that the inclusion of continuum mode-coupling effects severely increases the numerical effort, and is, in fact, not feasible in a straightforward manner for higher-order correlation functions.

Significant contributions of higher-order correlations with respect to photons can be expected, e.g., if one of the considered QD transitions is resonant with a cavity mode, thereby providing feedback of the emitted photons. However, for QD emission into a continuum of free-space modes, where photons disappear once emitted, corrections to the dynamical evolution of the photon-assisted polarization, introduced by higher order *photon correlations* are negligible. Nevertheless, *carrier correlations* can still play an important role, as we have pointed out in our previous work.<sup>15</sup> Especially in the regime of few emitters these correlations strongly dictate the carrier-photon dynamics and are indispensable for the description of single-QD luminescence.

The light-matter part of the Hamiltonian (A5) yields the time evolution

$$\begin{aligned} \left. \frac{d}{dt} C_{ijkl}^x \right|_{\mathcal{H}_{\text{LM}}} &= - \sum_{\xi} \delta_{il} \delta_{jk} [g_{\xi}^* (f_i^v - f_i^c) \Pi_{\xi,j} + g_{\xi} (f_j^v - f_j^c) \Pi_{\xi,i}^*] \\ &+ \sum_{\xi} [g_{\xi} \Pi_{\xi,lkji}^{c,*} + g_{\xi}^* \Pi_{\xi,ijkl}^c - g_{\xi} \Pi_{\xi,lkji}^{v,*} - g_{\xi}^* \Pi_{\xi,ijkl}^v]. \end{aligned} \quad (18)$$

The first line contains the factorized contributions of the expectation values  $\langle b_{\xi}^{\dagger} c_i^{\dagger} v_j^{\dagger} c_k c_l \rangle$  and  $\langle b_{\xi}^{\dagger} v_i^{\dagger} v_j^{\dagger} c_k v_l \rangle$ . The remaining correlation contributions  $\Pi_{\xi,ijkl}^c := \delta \langle b_{\xi}^{\dagger} c_i^{\dagger} v_j^{\dagger} c_k c_l \rangle$  and  $\Pi_{\xi,ijkl}^v := \delta \langle b_{\xi}^{\dagger} v_i^{\dagger} v_j^{\dagger} c_k v_l \rangle$  appear in the second line. Specifically,  $\Pi_{\xi,ijij}^{c/v} = -\Pi_{\xi,ijji}^{c/v}$  describe the correlated process of a photon-assisted polarization in presence of an additional carrier in the conduction- or valence-band, respectively. In a similar manner, equations for the intraband carrier correlations  $C_{ijkl}^c := \delta \langle c_i^{\dagger} c_j^{\dagger} c_k c_l \rangle$  and  $C_{ijkl}^v := \delta \langle v_i^{\dagger} v_j^{\dagger} v_k v_l \rangle$  can be obtained and are provided in Appendix B.

The before-mentioned natural truncation of the hierarchy of carrier operators becomes apparent in the time evolution of the mixed correlation functions  $\Pi_{\xi,ijkl}^c$  and  $\Pi_{\xi,ijkl}^v$ . To facilitate a better understanding, we provide a schematic explanation using the notation introduced in Sec. II. The quantities  $\Pi_{\xi,ijkl}^c$  and  $\Pi_{\xi,ijkl}^v$  are correlation functions  $\delta \langle M, N \rangle$  of the order  $M = 1$  and  $N = 2$ . The time evolution with respect to the

TABLE I. Overview of all relevant correlation functions for the semiconductor luminescence model discussed in Sec. IV.

		$N$		
		0	1	2
$M$	0	/	$\langle c^\dagger c \rangle, \langle v^\dagger v \rangle$	$\delta \langle c^\dagger v^\dagger cv \rangle, \delta \langle c^\dagger c^\dagger cc \rangle, \delta \langle v^\dagger v^\dagger vv \rangle$
	1	/	$\delta \langle b^\dagger v^\dagger c \rangle$	$\delta \langle b^\dagger c^\dagger v^\dagger cc \rangle, \delta \langle b^\dagger v^\dagger v^\dagger cv \rangle$
	2	$\langle b^\dagger b \rangle$	$\delta \langle b^\dagger bc^\dagger c \rangle, \delta \langle b^\dagger bv^\dagger v \rangle$	$\delta \langle b^\dagger bc^\dagger v^\dagger cv \rangle, \delta \langle b^\dagger bv^\dagger v^\dagger vv \rangle, \delta \langle b^\dagger bc^\dagger c^\dagger cc \rangle, \delta \langle b^\dagger b^\dagger v^\dagger v^\dagger cc \rangle$
	$\vdots$	$\vdots$	$\vdots$	$\vdots$

light-matter part of the Hamiltonian is given by

$$\left. \frac{d}{dt} \delta \langle 1, 2 \rangle \right|_{\mathcal{H}_{\text{LM}}} = \langle 0, 3 \rangle + \langle 2, 2 \rangle - \frac{d}{dt} \langle \delta \langle 1, 1 \rangle \rangle \langle 0, 1 \rangle - \delta \langle 1, 1 \rangle \frac{d}{dt} \langle 0, 1 \rangle. \quad (19)$$

Each term in this schematic representation may correspond to several contributions. The time derivative of the factorization is subtracted in the last line in order to obtain a correlation function [see Eq. (2)]. Due to the limitation to two carriers in the QD states the first term drops out, because it describes processes where three carriers are created or annihilated. Enforcing this property of the system requires the strict fulfillment of the additional condition

$$\delta \langle 0, 3 \rangle = -\delta \langle 0, 2 \rangle \langle 0, 1 \rangle - \langle 0, 1 \rangle \langle 0, 1 \rangle \langle 0, 1 \rangle, \quad (20)$$

which means that, in fact, *all* correlation functions up to  $N_{\text{max}} = 2$  must be taken into account. This is the explicit manifestation of what we referred to earlier as the enhancement of correlations due to the limited size of the system.

The remaining hierarchy in the photon operators is truncated at the desired level  $M_{\text{max}}$ . All terms appearing in the cluster expansion up to  $M_{\text{max}} = 2$  are summarized in Table I. Applying the cluster expansion to the remaining second term in Eq. (19) yields

$$\left. \frac{d}{dt} \delta \langle 1, 2 \rangle \right|_{\mathcal{H}_{\text{LM}}} = +\delta \langle 2, 2 \rangle + \delta \langle 2, 0 \rangle \delta \langle 0, 2 \rangle + \delta \langle 1, 1 \rangle \delta \langle 1, 1 \rangle + \delta \langle 2, 1 \rangle \langle 0, 1 \rangle - \frac{d}{dt} \langle \delta \langle 1, 1 \rangle \rangle \langle 0, 1 \rangle - \delta \langle 1, 1 \rangle \frac{d}{dt} \langle 0, 1 \rangle. \quad (21)$$

Explicitly performing the calculation behind this schematic representation leads to the following equations of motion:

$$\begin{aligned} & \left. \frac{d}{dt} \Pi_{\xi,ijkl}^c \right|_{\mathcal{H}_{\text{LM}}} \\ &= \left[ g_\xi f_i^c f_j^c f_j^v - g_\xi^* \Pi_{\xi,i} \Pi_{\xi,j} + g_\xi \mathcal{N}_{\xi,i}^c (f_j^c - f_j^v) \right. \\ & \quad \left. - g_\xi f_i^c \sum_\alpha C_{\alpha jj\alpha}^x \right] (\delta_{il} \delta_{jk} - \delta_{ik} \delta_{jl}) + g_\xi (1 + \mathcal{N}_\xi) C_{ijkl}^c \\ & \quad + g_\xi \mathcal{N}_\xi (C_{ijlk}^x - C_{ijkl}^x) + g_\xi \delta \langle b_\xi^\dagger b_\xi c_i^\dagger c_j^\dagger c_k c_l \rangle \\ & \quad + g_\xi \delta \langle b_\xi^\dagger b_\xi c_i^\dagger v_j^\dagger c_l v_k \rangle - g_\xi \delta \langle b_\xi^\dagger b_\xi c_i^\dagger v_j^\dagger c_k v_l \rangle \\ & \quad - g_\xi^* \delta \langle b_\xi^\dagger b_\xi v_i^\dagger v_j^\dagger c_k c_l \rangle, \end{aligned} \quad (22)$$

and similar equations can be given for  $\Pi_{\xi,ijkl}^v$  by exploiting the symmetries of the Hamiltonian.

It is worthwhile pointing out that the restriction to a certain system size fundamentally changes the structure of the underlying equations of motion. In Eq. (22), the uncommon product of three populations appears in the first line, originating from the subtraction of the factorization in the last line of Eq. (21) [from Eq. (17) one finds that there is a contribution  $\frac{d}{dt} \delta \langle 1, 1 \rangle \propto \langle 0, 1 \rangle \langle 0, 1 \rangle$ ]. In a system where the restriction to two carriers was lifted, these terms would be compensated by the factorization of the three-particle expectation value  $\langle 0, 3 \rangle$ , which would, in this case, have a nonzero contribution. In fact, this compensation is also known as the linked-cluster theorem.<sup>18</sup> Finally, the correlation function  $\delta \langle b_\xi^\dagger b_\xi v_i^\dagger v_j^\dagger c_k c_l \rangle$  in the last line of Eq. (22) can be attributed to spontaneous two-photon emission, recently demonstrated for a single-QD in a high- $Q$  photonic crystal nanocavity.<sup>53</sup>

Equations (16)–(22), together with the additional equations given in Appendix B, form a closed set of coupled nonlinear equations for the Hamiltonian dynamics. Before we turn to numerical results, we discuss the scattering and dephasing contributions to these equations.

## B. System-bath interaction

In Sec. III, we have discussed the reservoir-treatment of scattering and dephasing, as well as carrier pumping. In the equations of motion, these contributions are included via Lindblad terms in Eq. (14).

As we have briefly mentioned, a microscopic treatment of these processes is also possible and can be derived from a mixed basis of localized and extended states. For the quantum-well case, this has been performed by including the carrier-phonon interaction explicitly in the Hamiltonian.<sup>12,25</sup> However, this approach comes along with an additional hierarchy in the phonon operators that makes the classification of mixed correlation function containing carrier, photon, *and* phonon operators more difficult. Furthermore, including delocalized states of the two-dimensional WL continuum on the same level of complexity as the equations presented in Sec. IV A, i.e., by considering correlation functions of an order up to  $M_{\text{trunc}} = 2$  and  $N_{\text{max}} = 2$ , would involve nonlinearly coupled integrodifferential equations for correlation functions that carry several indices of continuum states. A numerical solution would currently be possible only for certain limiting cases. Therefore we base our approach for the inclusion of scattering and dephasing within the cluster expansion method on the Lindblad formalism. As a benefit, delocalized states enter the system dynamics only in the calculation of the



Lindblad rates, which can be obtained phenomenologically or from independent quantum-kinetic calculations.<sup>35,46,47,54–59</sup> In principle, the structure of the Lindblad formalism allows for a high degree of sophistication. For example, occupation-induced energy renormalizations due to the Coulomb interaction can be explicitly taken into account in the calculation of scattering, which then leads to different scattering rates for different configurations.<sup>35</sup> The influence of this effect is strongly entwined with the dynamics of the system. Especially at low WL carrier densities when screening is weak, the rates may differ significantly, and a study of the impact on the emission dynamics of a single QD in a microcavity could prove interesting for future studies.

We now turn to the equations of motion. By evaluating the second line of Eq. (14), we can calculate the contributions for scattering, pumping, and cavity losses.

### 1. Intraband scattering

For the scattering between the bound QD states  $\mu$  and  $\nu$  in the conduction band, we obtain

$$\begin{aligned} \left. \frac{d}{dt} \langle A \rangle \right|_{\text{scatt}} &= \sum_{\substack{\mu \neq \nu \\ \mu, \nu \in \{s, p\}}} \frac{\gamma_{\mu\nu}^{cc}}{2} (\langle [c_\mu^\dagger c_\nu, A] c_\mu^\dagger c_\nu \rangle + \langle c_\nu^\dagger c_\mu [A, c_\mu^\dagger c_\nu] \rangle), \end{aligned} \quad (23)$$

where we have identified  $\sigma_\eta$  by  $c_\mu^\dagger c_\nu$ , and the Lindblad rates  $\gamma_\eta$  by the intraband scattering rates  $\gamma_{\mu\nu}^{cc}$ . The resulting change in the single-particle population  $f_\nu^c = \langle c_\nu^\dagger c_\nu \rangle$  due to intraband scattering,

$$\begin{aligned} \left. \frac{d}{dt} f_\nu^c \right|_{\text{scatt}} &= S_\nu^{\text{in}} (1 - f_\nu^c) - S_\nu^{\text{out}} f_\nu^c \\ &\quad + \sum_{\mu \neq \nu} (\gamma_{\nu\mu}^{cc} - \gamma_{\mu\nu}^{cc}) C_{\nu\mu\nu\mu}^c, \end{aligned} \quad (24)$$

takes on the form of a Boltzmann-like collision term (first line), consisting of in- and out-scattering contributions with the corresponding rates  $S_\nu^{\text{in}} = \sum_{\mu \neq \nu} \gamma_{\nu\mu}^{cc} f_\mu^c$  and  $S_\nu^{\text{out}} = \sum_{\mu \neq \nu} \gamma_{\mu\nu}^{cc} (1 - f_\mu^c)$ , as well as correlation contributions beyond the single-particle description (second line). It is evident that the total carrier number is preserved, i.e.,  $\frac{d}{dt} \sum_\nu f_\nu^c = 0$ , reflecting the trace-conserving property of the Lindblad formulation that we have already discussed in the context of Eq. (11).

If carrier correlations  $C_{\nu\mu\nu\mu}^c$  are neglected in Eq. (24), only populations of single-particle states  $f_\nu^c$  are taken into account. These populations are obtained by averaging over all configurations containing a carrier in the state  $\nu$ . Due to this averaging, the single-particle description is not able to distinguish between different configurations with an occupation of the state  $\nu$  and can, thereby, account for the Pauli exclusion principle only in an averaged sense. Consider, for example, the carrier relaxation in the conduction band. The configurations  $|1X_p\rangle$ ,  $|0X_p\rangle$ , and  $|2X_{sp}\rangle$  are valid initial configurations for a  $p$ -to- $s$  electron scattering process, although the Pauli exclusion principle forbids a carrier transition for the latter, because the

$s$  shell already contains one carrier. Thus, in this case, the single-particle description allows for relaxation and attributes for dephasing, whereas an exact configuration-based treatment does not. Especially for few-emitter systems, this deficiency of the single-particle description (sometimes called ‘‘collision approximation’’ of carrier correlations) should be avoided by considering the carrier correlations in Eq. (24).

The inclusion of scattering processes introduces a natural source of dephasing for all correlation functions. The scattering contribution to the equations of motion of the photon-assisted polarization,

$$\left. \frac{d}{dt} \Pi_{\xi, \nu} \right|_{\text{scatt}} = -\Gamma_\nu \Pi_{\xi, \nu} - \frac{1}{2} \sum_{\mu \neq \nu} (\gamma_{\nu\mu}^{cc} - \gamma_{\mu\nu}^{cc}) \Pi_{\xi, \mu\nu\nu\mu}^c, \quad (25)$$

includes a population-dependent dephasing rate  $\Gamma_\nu = \frac{1}{2} (S_\nu^{\text{in}} + S_\nu^{\text{out}})$ , instead of a constant rate  $\Gamma$  that is frequently used in the literature. To study the influence of correlations, it is crucial to account for their proper dephasing, because it determines the timescale on which correlations are damped out. We have shown in Ref. 15 that the influence of the carrier correlations on the luminescence dynamics can be strong if no dephasing is used at all, while a small constant dephasing of the interband correlation function in the  $\mu\text{eV}$  regime already leads to a complete damping towards an uncorrelated system on a timescale of several 100 ps. To make quantitative predictions, a consistent treatment of dephasing with correct rates for the different correlation functions is important. The dynamics of the interband carrier correlations due to intraband scattering introduced by the Lindblad term (23) is given by

$$\begin{aligned} \left. \frac{d}{dt} C_{ijkl}^x \right|_{\text{scatt}} &= - \sum_{\substack{\mu \neq \nu \\ \mu, \nu \in \{s, p\}}} \frac{\gamma_{\mu\nu}^{cc}}{2} \{ C_{ijkl}^x (\delta_{i\mu} + \delta_{k\mu}) \\ &\quad - 2 [f_\mu^c f_j^v (\delta_{i\mu} \delta_{k\mu} - \delta_{i\nu} \delta_{k\nu}) \delta_{jl} + C_{\mu j \mu l}^x \delta_{i\nu} \delta_{k\nu}] \\ &\quad - 2 [(f_\mu^c (1 - f_i^c) - C_{\mu i i \mu}^c) \delta_{i\nu} \\ &\quad - (f_i^c (1 - f_\nu^c) - C_{i \nu \nu i}^c) \delta_{i\mu}] f_j^v \delta_{ik} \delta_{jl} \}, \end{aligned} \quad (26)$$

from which we obtain, using  $C_{spsp}^c = C_{psps}^c = -C_{spps}^c = -C_{psps}^c$ , the following sum rule:

$$\left. \frac{d}{dt} (C_{ssss}^x + 2C_{psps}^x) \right|_{\text{scatt}} = 0. \quad (27)$$

Thus both correlation functions  $C_{ssss}^x$  and  $C_{psps}^x$  are not independent quantities but are linked by the scattering process they represent. Obviously this property cannot be fulfilled by a simpler approach, where equal and constant rates  $\Gamma$  are used to describe the dephasing of both correlation functions.

### 2. Pumping

In a typical situation, carriers are excited in the barrier states and subsequently captured into the QD states. We describe this by a simultaneous generation/annihilation of carriers in the conduction/valence band  $p$  state, which is assumed to persist during the pump pulse and to rapidly disappear afterwards. Specifically, we consider a time-dependent capture rate  $P(t)$  following a Gaussian-shaped pump pulse. The corresponding

Lindblad contribution to the equation of motion reads

$$\frac{d}{dt} \langle A \rangle \Big|_{\text{pump}} = \frac{P(t)}{2} (\langle [v_p^\dagger c_p, A] c_p^\dagger v_p \rangle + \langle v_p^\dagger c_p [A, c_p^\dagger v_p] \rangle). \quad (28)$$

This treatment of the pump process leads to an automatic built-up of correlation functions, e.g., for correlations between conduction- and valence-band carriers in the  $p$  shell:

$$\frac{d}{dt} C_{pppp}^x \Big|_{\text{pump}} = P(t) (f_p^v - f_p^c) [C_{pppp}^x + (1 - f_p^c) f_p^v]. \quad (29)$$

This way, initial conditions for correlations do not have to be calculated separately by considering a quasiequilibrium initial-state population that is defined by a total carrier density and a temperature.<sup>14,15</sup>

It is worth noting that it is particularly the pair-wise generation of electrons and holes that leads to the generation of certain electron-hole correlations in the system. Furthermore, since the recombination also destroys electrons and holes pairwise, only configurations with an equal number of electrons and holes appear in the system dynamics. Thereby, charged excitonic configurations are excluded. Alternative pump schemes can be considered<sup>34,40</sup> in which electrons and holes are captured independently. The implications are worth a separate discussion, which we give in Sec. VII.

### 3. Cavity losses

In Sec. VI, we show results for a QD in a microcavity. The latter provides a three-dimensional confinement of the electromagnetic field, leading to a spectrum of well-separated cavity modes. This allows for the situation, in which only a single mode  $\bar{\xi}$  is resonant with the  $s$ -exciton transition of the QD. Nevertheless, nonresonant modes  $\xi \neq \bar{\xi}$  are weakly coupled to QD transitions and introduce dissipation on a nanosecond timescale.

To account for a finite lifetime of the resonant mode, we introduce the following Lindblad contribution:

$$\frac{d}{dt} \langle A \rangle \Big|_{\text{cav}} = \frac{\kappa_{\bar{\xi}}}{2} (\langle [b_{\bar{\xi}}^\dagger, A] b_{\bar{\xi}} \rangle + \langle b_{\bar{\xi}}^\dagger [A, b_{\bar{\xi}}] \rangle), \quad (30)$$

where the photon loss rate  $\kappa_{\bar{\xi}}$  is directly connected to the quality factor  $Q = \omega_{\bar{\xi}}/\kappa_{\bar{\xi}}$  of the cavity mode  $\bar{\xi}$  at the energy  $\omega_{\bar{\xi}}$ .

Note that this contribution has a similar structure as the one for the carrier scattering (23), but now contains system operators acting only on the photonic degrees of freedom and leading to transitions between states involving  $n$  and  $n - 1$  photons in the mode  $\bar{\xi}$ . The contribution to the equations of motion leads to a damping of correlations at a rate  $M\kappa_{\bar{\xi}}/2$ ,

$$\frac{d}{dt} \delta \langle (b_{\bar{\xi}}^\dagger)^p (b_{\bar{\xi}})^q \mathcal{Q} \rangle \Big|_{\text{cav}} = -M \frac{\kappa_{\bar{\xi}}}{2} \delta \langle (b_{\bar{\xi}}^\dagger)^p (b_{\bar{\xi}})^q \mathcal{Q} \rangle, \quad (31)$$

where  $M = p + q$  is the order of the corresponding correlation function with respect to the photon operators, independent of further carrier operators  $\mathcal{Q}$  contained in the correlation function. Thus photon correlations get more strongly damped in the presence of a lossy cavity and, even more so, with

increasing order. This plays an important role in the truncation of the hierarchy within the cluster expansion approach and is demonstrated in Sec. VI.

### C. Luminescence dynamics and spectrum

The luminescence dynamics is determined by the change of the mean photon number  $\mathcal{N}_{\bar{\xi}}$  for which the equation of motion reads

$$\left( \frac{d}{dt} + \kappa_{\bar{\xi}} \right) \mathcal{N}_{\bar{\xi}} = 2 \text{Re} \sum_{\nu} g_{\bar{\xi}}^* \Pi_{\bar{\xi}, \nu}. \quad (32)$$

The only contributions to this equation arise from the light-matter interaction and the cavity losses in Eq. (30). One can see that cavity losses lead to a decrease of the mean photon number, while spontaneous and stimulated emission and absorption due to the emitter are expressed in terms of the sum over the photon-assisted polarizations over all bound QD states.

In the absence of a cavity, emission into the continuum of free space modes takes place, and the corresponding luminescence spectrum  $I(\omega, t)$  is given by

$$I(\omega, t) = 2 \text{Re} \sum_{\nu, \xi} |g_{\xi}|^2 \Pi_{\xi, \nu} \Big|_{|q|=\frac{\omega}{c}}. \quad (33)$$

Note that from here on, we consider all polarization-like quantities to be rescaled with the light-matter coupling strength  $g$  in order to have the square of the coupling constant appear in the equations; for details, we refer to Ref. 15. Here, the sum runs over wave vectors with the same photon energy irrespective of the direction of the wave vector. When studying time-resolved photoluminescence, the spectral information is discarded by integration over all frequencies, i.e.,

$$I(t) = \int d\omega I(\omega, t). \quad (34)$$

### V. PHOTOLUMINESCENCE INTO FREE SPACE

We first present numerical results for the luminescence from a single QD into a continuum of modes, i.e., free-space emission. Here, the equation-of-motion approach can play out its full advantage, because the large Hilbert space associated with a continuum of modes prohibits a direct solution of the von-Neumann equation. The particular four-level QD is used that we have introduced in the previous section. The luminescence spectra and the time-resolved photoluminescence decay provide direct insight into both the physical system and the underlying mechanism of the FSH approach. Furthermore, comparing with results from the cluster expansion method enables us to gain an understanding how the approximate treatment of the carrier degrees of freedom leads to an effective “mean-field”-like approximation of the exact result and the limitations of this description. The frequency-resolved and time-dependent luminescence spectra are calculated from Eq. (33).

In Fig. 4, we show four series of luminescence spectra from the emission 10, 20, 30, and 50 ps after the start of the time evolution. Continuum-state carriers are excited by a laser pulse and are subsequently captured pairwise into the QD  $p$  states. A separate discussion of the particularities and

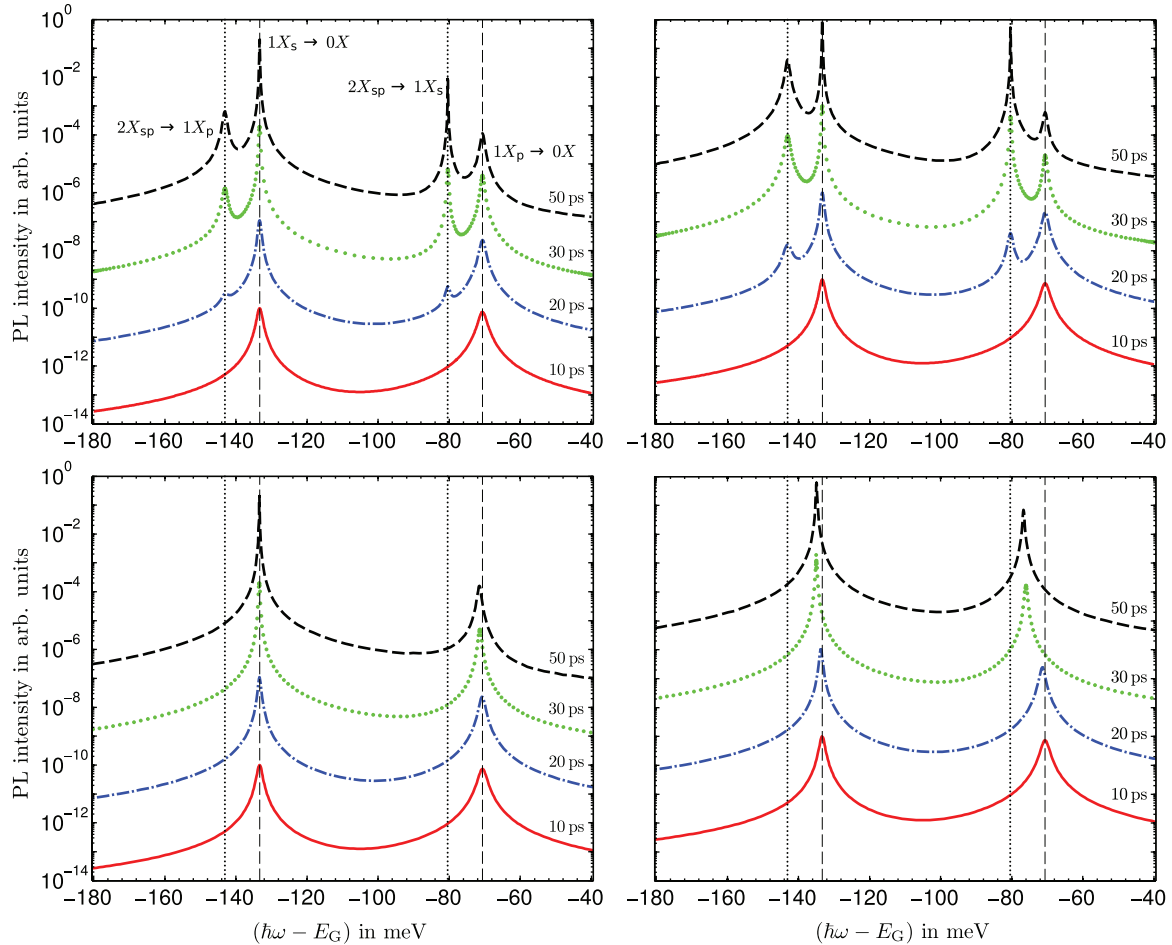


FIG. 4. (Color online) Frequency-resolved photoluminescence spectra for the emission into a continuum of modes. Compared are FSH (top) and doublet-level cluster expansion (bottom) results after a weak (left,  $P_{\text{total}} = 0.1$ ) and strong (right,  $P_{\text{total}} = 1.0$ ) excitation pulse. Spectra are shown after 10 (solid line), 20 (dash-dotted), 30 (dotted), and 50 (dashed) ps of the time evolution. The excitation pulse is centered at 25 and 10 ps in width. The spectra have been rescaled for better visibility. In order to be able to compare absolute heights, the scaling factors are required. Typical relaxation times for electrons in the conduction and valence bands are used:  $\gamma_{sp}^{cc} = 1.07/\text{ps}$ ,  $\gamma_{ps}^{cc} = 0.02/\text{ps}$ ,  $\gamma_{sp}^{vv} = 0.13/\text{ps}$ , and  $\gamma_{ps}^{vv} = 0.59/\text{ps}$ . The peak height of the top right spectrum after 50 ps has been set to unity. Relative to this, in all panels, the spectra after 40, 30, 20, and 10 ps have been scaled by  $0.76$ ,  $0.31$ ,  $0.02$ , and  $1.4 \times 10^{-5}$ .

implications of pairwise carrier generation is the topic of Sec. VII. The Gaussian pulse is centered at 25 ps and has a width of 10 ps (FWHM) and a dimensionless pulse area of  $P_{\text{total}}$ . The spectra in the left panel correspond to weak excitation with  $P_{\text{total}} = 0.1$ , whereas the right panel shows results after strong excitation with  $P_{\text{total}} = 1$ . Upper and lower panels compare results from the FSH method for  $M_{\text{trunc}} = 1$ , and the doublet-level cluster expansion with  $(N + M)_{\text{trunc}} = 2$ , respectively.

We first provide an explanation of the FSH results. Since the FSH method contains an exact treatment of the carrier degrees of freedom, the resulting (multi)exciton lines appear at renormalized energies that are equivalent to those obtained from a diagonalization of the carrier and Coulomb Hamiltonian with the “full configuration interaction” procedure. The position of the lines is fixed, and their intensity in the spectrum is determined by the probability of the corresponding transition taking place. Four peaks are visible, which correspond to the four possible recombination channels of the excited QD system, namely the decay to the ground state from the  $s$  and

$p$  excitons, as well as the  $s$  and  $p$  recombination from the  $s$ - $p$ -biexciton configuration. The  $s$  and  $p$  recombination are separated by approximately 63 meV in the spectrum due to the level spacing of the single-particle states and direct (Hartree) interaction. The Coulomb Hamiltonian introduces a further splitting, if the recombination takes place in the presence of another electron-hole pair in the other shell. The splitting between the  $2X_{sp} \rightarrow 1X_{s/p}$  and the  $1X_{s/p} \rightarrow 0X$  transitions is mainly determined by the Coulomb  $s$ - $p$ -exchange interaction and gives rise to a detuning of  $2V_{spsp}$ , which amounts approximately to 9.8 meV.

Because all recombination channels are spectrally separated, it is possible to infer information about the carrier dynamics from the time-dependent spectra in Fig. 4. The following discussion is valid for both upper panels, as the situation is similar for weak and strong excitation. In the lowermost spectrum in each panel, corresponding to the beginning of the excitation pulse, only signatures of  $s$ - and  $p$ -exciton emission are visible. Because excitation is still weak, relaxation and recombination are by far the fastest processes

in the system, so that excitations decay before a biexciton can form. The second spectra (dotted lines) depict the situation just before the peak of the excitation pulse. The now faster refilling of the  $p$  states already leads to weak signatures of the biexciton emission. One can also see that the  $s$ -exciton emission clearly dominates over that of the  $p$  exciton. This effect becomes even more obvious in the spectra at later times and is explained by the scattering processes between  $s$  and  $p$  shells; at a considered temperature of 120 K, down-scattering from  $p$  to  $s$  shell is much faster than the reverse process and offers a fast second channel in addition to the direct recombination, through which the  $p$  exciton can decay.

Before we discuss the results of the cluster expansion, we elaborate on the origin of the spectral splitting between exciton and biexciton emission in the formalism. The biexciton recombination process is described by the expectation value  $\langle b_\xi^\dagger X_s X_p^\dagger X_p \rangle$ . Here, exciton operators  $X_i^\dagger = c_i^\dagger v_i$  have been used to express the recombination process of an exciton in the  $s$  shell in the presence of a second exciton in the  $p$  shell (equivalently,  $p$ -shell recombination in the presence of an  $s$ -shell exciton is given by a similar expression). Normal ordering yields

$$\begin{aligned} \langle b_\xi^\dagger X_s X_p^\dagger X_p \rangle &= \langle b_\xi^\dagger v_s^\dagger c_s c_p^\dagger v_p v_p^\dagger c_p \rangle \\ &= \langle b_\xi^\dagger v_s^\dagger c_s c_p^\dagger c_p \rangle - \langle b_\xi^\dagger v_s^\dagger c_p^\dagger v_p v_p^\dagger c_p c_s \rangle. \end{aligned} \quad (35)$$

The assumption of pairwise carrier generation and the resulting limitation to the six possible configurations shown in Fig. 2 imply that the second term must be zero (annihilation of three carriers is not possible under the described circumstances), so that the biexciton recombination process is actually described by the quantity  $\langle b_\xi^\dagger v_s^\dagger c_s c_p^\dagger c_p \rangle$ . This can readily be understood, as the presence of two carriers in the conduction-band  $s$  and  $p$  states automatically implies their absence in the valence-band states. At this point, the limitation to account for scattering processes that leave the total number of carriers in the localized states constant constitutes a significant simplification of the FSH method. In the more general case, which is the topic of Sec. VII, equations of motion for correlation functions containing up to  $2N_{\max} = 8$  carrier and  $M_{\text{trunc}} = 1$  photon operators are required.

We now turn to the results of the cluster expansion method (lower two panels). Here, the truncation is performed at the level  $(N + M)_{\text{trunc}} = 2$ , implying that all correlation functions containing more than four carrier operators are approximated as zero. Correlation functions  $\Pi_{\xi,ijkl}^{c/v}$  responsible for biexcitonic emission, as they appear in the spectra obtained from the FSH, are not included in the theory at the doublet level. As a result of the truncation, the cluster expansion method performs a compensation in a mean-field-like fashion:<sup>50</sup> peaks appear at the  $s$ - and  $p$ -exciton transitions at energies that are renormalized proportionally to the single-particle electron and hole populations in the QD states. With increasing excitation the resonances are tuned *continuously* towards the energies of the multiexciton configurations that are visible in the full theory. The amount of the shift results from the singlet contribution  $\sum_\mu V_{i\mu i\mu} (1 + f_\mu^c - f_\mu^v)$  in the dynamical equation for the photon-assisted polarization  $\Pi_{\xi,s/p}$  responsible for the  $s$ -( $p$ -)shell recombination. The exact Coulomb-renormalized

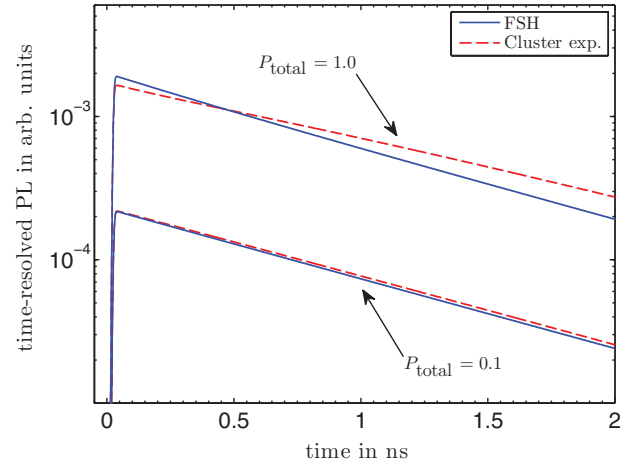


FIG. 5. (Color online) Time-resolved photoluminescence for the results shown in the previous figure.

energies of the four recombination channels are shown as vertical lines as a guide to the eye to better visualize the shift. This effect can also be observed in the absorption spectra shown in Ref. 51, where results from calculations on the mean-field and two-particle correlation level are compared. Spectral line shifts, though not the main focus of that publication, are prominent especially in the first case and are reduced by the important step to include two-particle correlations.

Complementary information, which turns out less sensitive to the approximate treatment of carrier correlations, is provided by the time-resolved photoluminescence, which is obtained by integrating the spectrum over all energies at every point in time. The result for the discussed four situations is shown in Fig. 5, where curves from the FSH and cluster expansion methods are compared. For weak excitation ( $P_{\text{total}} = 0.1$ ), both results are in good agreement, demonstrating that the “interpolation” performed by the cluster expansion on the doublet level provides indeed a good approximation of the total photon emission. At high excitation ( $P_{\text{total}} = 1.0$ ), when additional configurations become increasingly important, deviations appear. Strong line shifts are observed in the corresponding spectra (lower right panel in Fig. 4) in order to mimic the dominant emission from the filled QD configuration at the  $p$  shell resonance. In this regime, the doublet-level cluster expansion method breaks down and unphysical results, like negative populations may occur.

The interpolation of the transition energies in the doublet-level cluster expansion method leads to a problem in the presence of a high- $Q$  resonator. The narrow line width associated with the cavity mode makes the light emission very sensitive to shifts of the emission lines, leading to a population-dependent overlap between QD transition and mode. This artificial situation is discussed in detail in Sec. VI.

The final aspect of the spectra that requires additional explanation regards the line widths of the different transitions. We have explained in the context of Eq. (12) that scattering processes lead to dephasing of optical transitions if they act on either the initial and/or final state of that transition.<sup>34,40</sup> The strength of the underlying dephasing manifests itself in the line widths in the emission spectrum. For example, the  $s$  exciton to ground-state transition is subject to the  $p$ -shell

carrier generation process as well as the up-scattering of electrons and holes from  $s$  to  $p$  states. While the latter is very weak, the pump process is responsible for the line broadening of the corresponding peak. After the pump pulse is over, the line clearly narrows (compare the spectra at 10 and 50 ps). The situation is similar for the  $p$ -exciton-to-ground-state transition, which is affected by the pump process in the same way, but is additionally dephased by the fast carrier relaxation from  $p$  to  $s$  states. In contrast to the previously discussed transition, the line of the corresponding peak is not narrowed after the excitation pulse is over.

The effect of carrier relaxation is reversed for the biexciton emission lines. Since for the considered QD system, the initial configuration of this recombination process is the completely filled QD, only the final configuration, which is either the  $s$  or the  $p$  exciton, can be involved in carrier scattering. For the  $p$  exciton, this is the fast  $p$ -to- $s$  relaxation, while for the  $s$  exciton, it is the much slower  $s$ -to- $p$  up-scattering process. Accordingly, the line width of the  $2X_{sp} \rightarrow 1X_s$  is significantly smaller than that of the  $2X_{sp} \rightarrow 1X_p$  transition. The impact of the dephasing reaches even deeper than its reflection in the transition line widths, and the final point we would like to discuss in the context of the spectra are the relative intensities of the two biexciton emission channels. Recombination at the  $s$  shell leaves behind a  $p$  exciton. As we have discussed before, this is subject to strong dephasing due to carrier relaxation. Recombination at the  $p$  shell, on the other hand, leaves behind the  $s$  exciton, which is only weakly dephased in the absence of pumping. Thus the photon-assisted polarization that drives the transition process is damped more strongly in the first case, which is clearly reflected by the higher peak in the spectrum at 50 ps after the pump pulse has ended.

## VI. NUMERICAL RESULTS FOR A SINGLE QD IN A MICROCAVITY

Now we turn to the situation in which a single-QD emitter is embedded in a resonator structure and coupled to a single high- $Q$  mode of that resonator. In contrast to the free-space emission considered in the previous section, the cavity strongly enhances the resonant emission from the QD. We will demonstrate that the resulting sensitivity to the resonance condition can lead to an enhancement of artifacts introduced

by the truncation of the hierarchy of equations of motion. The limited size of the Hilbert space now facilitates a direct solution of the vNL equation (13), which is exact, and against which we check the validity of (i) the FSH method, where carrier degrees of freedom are represented by a closed set of carrier correlation functions, plus the corresponding correlations augmented by photon operators up to order  $M_{\text{trunc}}$ , and (ii) the approximate treatment of carrier and photon degrees of freedom according to the conventional cluster expansion method at the doublet level  $(N + M)_{\text{trunc}} = 2$ .

We consider the  $s$ -exciton transition to be resonant with a single cavity mode, and a corresponding light-matter coupling strength of  $g = 0.01/\text{ps}$ . The pump process is modeled like in Sec. V [a Gaussian pulse centered at 25 and 10 ps of width (FWHM)] with a total area of  $P_{\text{total}} = 0.5$ . Typical relaxation times for electrons in the conduction and valence bands are used:  $\gamma_{sp}^{cc} = 1.07/\text{ps}$ ,  $\gamma_{ps}^{cc} = 0.02/\text{ps}$ ,  $\gamma_{sp}^{vv} = 0.13/\text{ps}$ , and  $\gamma_{ps}^{vv} = 0.59/\text{ps}$ .

In analogy to the discussion in Sec. IV C, we can infer that the luminescence dynamics follows from Eq. (33), when only a single mode  $\xi$  is considered. We drop the mode index in the remainder of this section. This leads to the expression

$$I(t) = 2|g|^2 \text{Re} \sum_v \Pi_v. \quad (36)$$

For a light-matter coupling strength of  $g = 0.01/\text{ps}$  and a cavity loss rate of  $\kappa = 0.1/\text{ps}$  ( $Q \approx 20\,000$  for a cavity mode wavelength of 915 nm), the time-resolved photoluminescence at the cavity resonance is shown in Fig. 6(a). The FSH method, which treats the electronic degrees of freedom exact and the photonic degrees of freedom up to second order ( $M_{\text{trunc}} = 2$ ), is in excellent agreement with the exact solution of the vNL equation (symbols). The solid line represents the cluster expansion at the doublet level  $(N + M)_{\text{trunc}} = 2$  and is found to exhibit a peculiar oscillatory behavior that strongly deviates from the exact result. The reason lies in the fact that, at this level of approximation, the transition energies are not fixed but are renormalized as a function of the carrier populations, as it was demonstrated in Sec. V. With the cavity tuned to the properly renormalized energy of the exciton transition, this transition comes into resonance as the *mean* QD carrier occupancy increases. With the onset

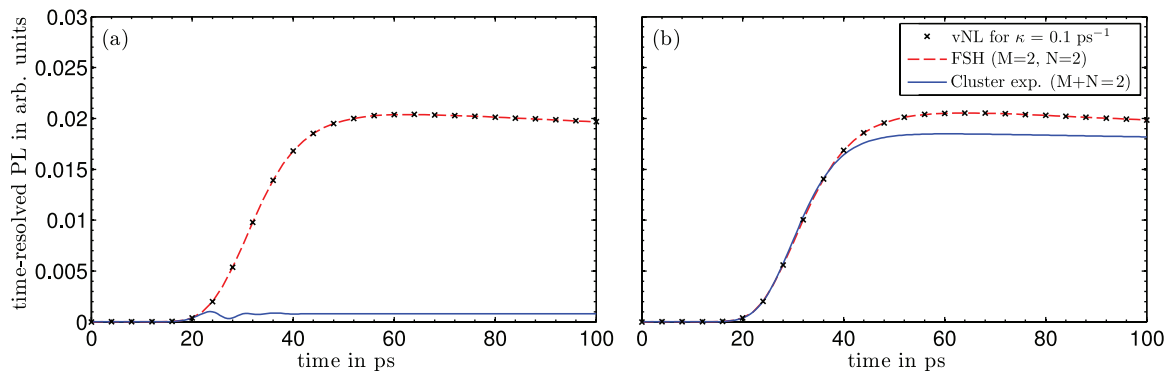


FIG. 6. (Color online) (a) Time-resolved photoluminescence at the cavity-mode frequency. Results obtained from the FSH (dashed lines) and doublet-level cluster expansion (solid lines) methods are compared to the exact solution (symbols) of the vNL equation. (b) Displays the same results under the omission of Coulomb interaction, see text.

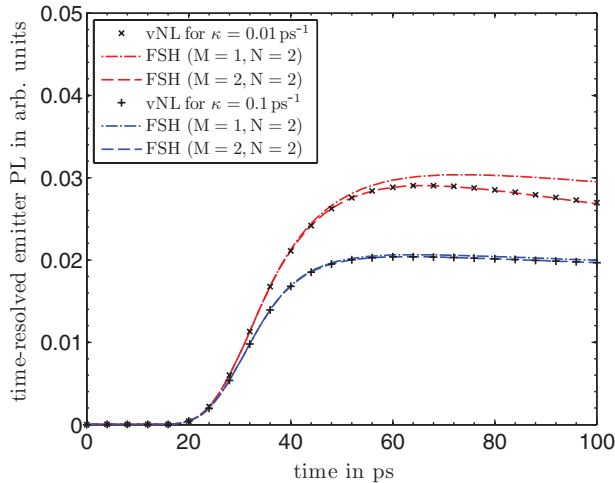


FIG. 7. (Color online) Comparison between the solution of the von-Neumann equation (symbols) and the FSH method for the time evolution of the single-QD photoluminescence. For all curves a light-matter coupling strength of  $g = 0.01/\text{ps}$  is used. The red lines and crosses correspond to the results for cavity losses at a rate  $\kappa = 0.01/\text{ps}$ . In comparison to the red curves,  $\kappa = 0.1/\text{ps}$  is used for the blue lines and plus symbols. The various line styles show the results of the FSH method obtained at different truncation levels with respect to the photonic hierarchy.

of emission, the QD is depopulated, which, in turn, reduces the renormalization and brings the exciton transition out of resonance again. This leads to an initial oscillatory behavior and finally to a strongly suppressed emission due to the reduced spectral overlap between emitter and cavity mode. This picture is supported by a comparative calculation where the influence of Coulomb interaction is neglected, shown in Fig. 6(b). In this case, exciton and biexciton recombination take place at the same energy, so that the shifting of the transition lines is artificially suppressed in the results of the cluster expansion method.

In Fig. 7, we study the influence of the truncation level in the photonic degrees of freedom when using the FSH method. The blue set of curves and plus symbols correspond to the parameters used in Fig. 6, the crosses and red set of curves depict the case of a cavity with an exaggeratedly long storage time of photons ( $\kappa = 0.01/\text{ps}$ ,  $Q \approx 200\,000$ ). For the  $Q \approx 20\,000$  cavity, a truncation of the photon hierarchy at the  $M_{\text{trunc}} = 1$  level (dash-dotted line) can hardly be distinguished from the results for  $M_{\text{trunc}} = 2$  (dashed line). The reason lies in the dephasing of these correlations due to the dissipation of photons from the cavity according to Eq. (31). In the higher- $Q$  cavity, the dephasing is significantly weakened, thereby strengthening the impact of photon correlations. Thus, the calculation for  $M_{\text{trunc}} = 1$  yields a visibly less accurate description of the time-resolved photoluminescence than the  $M_{\text{trunc}} = 2$  calculation. In the well-known manner of the cluster expansion, the level of truncation depends on the strength of correlations, as well as on the quantities of interest.

In this section, we have demonstrated that the FSH method yields an accurate description of the system dynamics and can overcome the limitations inherent to the cluster expansion

method at the doublet level. The results were obtained for a pairwise carrier generation process, which greatly simplifies the hierarchy of equations of motion. A generalization of the carrier generation is the topic of the next section.

## VII. CORRELATED AND UNCORRELATED CARRIER GENERATION

Up to this point, we have considered pair-wise capture of carriers from the continuum states into the localized  $p$  states of the QD, as well as QD-carrier-number conserving scattering processes, see Sec. IV. This implies full correlation between the generated electrons and holes. Since the optical recombination also acts pairwise, the dynamics of the considered QD system is completely determined by the smaller subset of configurations shown in Fig. 2. In this sense, the above approximations provide a convenient way to reduce the numerical effort of the discussed theoretical approach. In general, it would be desirable to model optical excitation of the continuum states and subsequent capture into localized states microscopically. For this, we expect only partial correlations between the generated electrons and holes. Some evidence for this picture is provided in Ref. 35, where it has been demonstrated that the independent capture of electrons and holes, which leads to a charging of the QD, is compensated by Coulomb interaction effects favoring the capture of additional carriers of the opposite charge.

In this section, we address the differences between correlated and uncorrelated electron-hole capture into the QD, as well as its reflection in the carrier correlations. Like in Sec. VI, we consider a single QD coupled to the single mode of the confined electromagnetic field for which we can access the full solution directly from the vNL equation.

In Fig. 8, the dynamical behavior after pulsed excitation is compared for correlated and uncorrelated excitation. The first is realized by using Eq. (28), while independent capture of electrons and holes into the QD  $p$ -states is accomplished by the Lindblad term:<sup>34,40</sup>

$$L_{\text{capt}}\rho = \frac{\gamma^{\text{in}}}{2}(2c_p^\dagger\rho c_p - c_p c_p^\dagger\rho - \rho c_p c_p^\dagger + 2v_p\rho v_p^\dagger - v_p^\dagger v_p\rho - \rho v_p^\dagger v_p). \quad (37)$$

We use a set of parameters that approximately describes the situation in current state-of-the-art single-QD laser devices:<sup>34,60</sup> light-matter coupling strength  $g = 0.1/\text{ps}$ , and a cavity loss rate of  $\kappa = 0.2/\text{ps}$  ( $Q \approx 10\,000$ ). The cavity mode is resonant with the  $1X_s$  exciton transition. The area of the pump pulse is  $P_{\text{total}} = 0.5$ .

The time-resolved photoluminescence (PL) at the cavity mode frequency is shown in the top row. Also added are the results of a calculation using the FSH method up to the  $M_{\text{trunc}} = 2$  level (dashed line) to enable a direct comparison. For the chosen parameter regime, which represents a QD-cavity system with a high coupling strength, the exact results (symbols) are very well reproduced. Results after correlated (left) and uncorrelated (right) excitation are qualitatively very similar. The PL intensity is, however, reduced in the latter case due to the build-up of configurations that are optically dark or inefficient. In case of pairwise excitation, the recombination

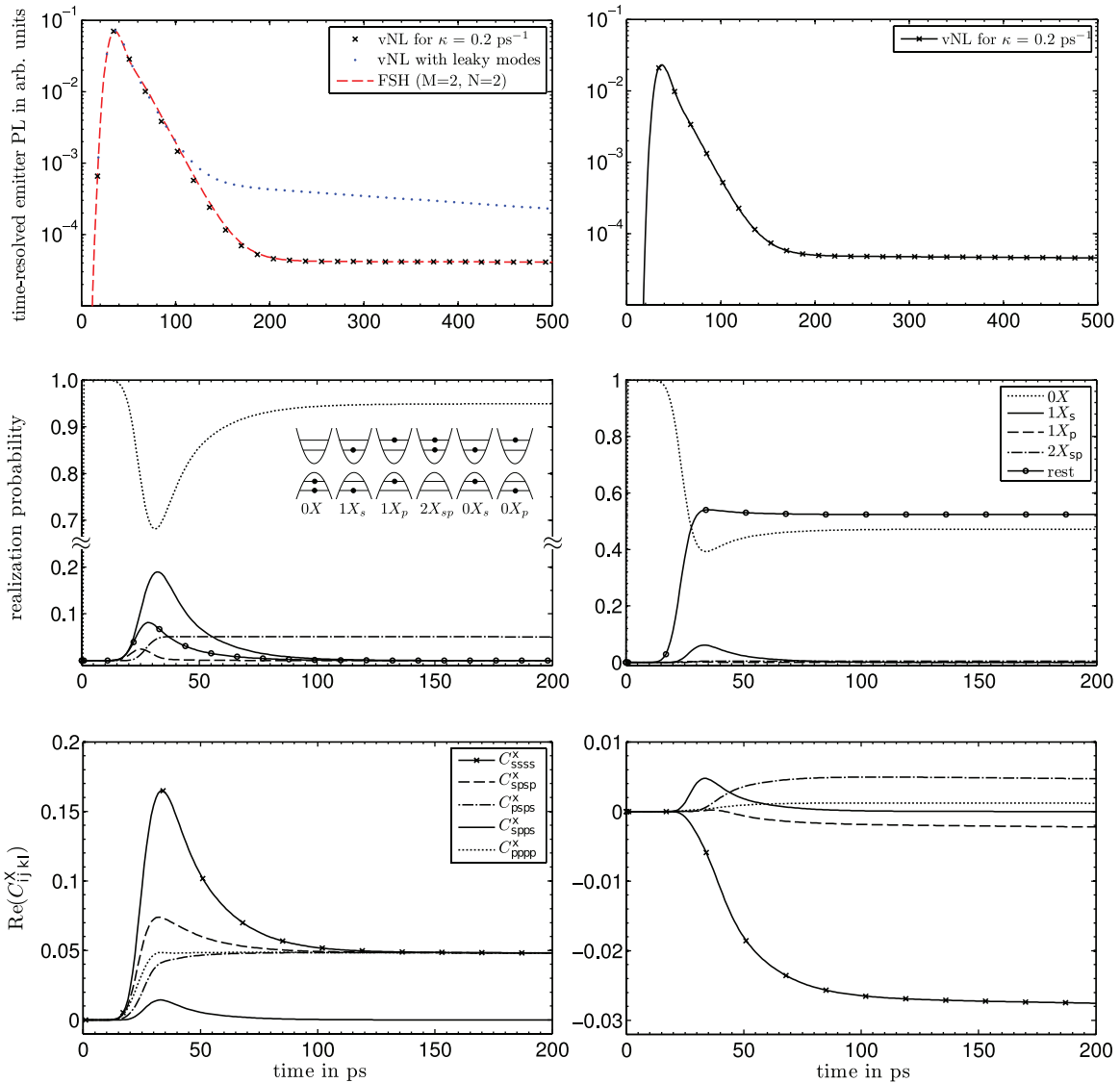


FIG. 8. (Color online) Comparison between the system behavior after correlated (pairwise) excitation (left) and uncorrelated (independent) carrier capture (right). (Top) Time-resolved PL on a time scale of 0.5 ns. In case of correlated excitation, the result of the vNL equation (symbols) is compared to that of the FSH method (dashed line). The dotted line corresponds to a calculation where an additional Lindblad term is used to account for leaky-mode losses at a rate of  $1/\text{ns}$ . (Middle) Realization probabilities for selected configurations. In case of uncorrelated carrier capture, 16 configurations are possible instead of six. Therefore the “rest” encompasses different configurations on the left and right. (Bottom) Real part of the interband carrier correlation function. The interpretation of these quantities is explained in the text.

dynamics is driven by the decay of the  $1X_s$  exciton during the first 180 ps. Subsequently, the photoluminescence quickly takes on a constant value. The combination of  $p$ -shell carrier generation and QD relaxation leads to the build-up of several configurations. For the considered spin-polarized excitation, we find the  $s$  and  $p$  excitons as well as the  $sp$  biexciton. The dynamical behavior of realization probabilities for these configurations is depicted in the middle row in Fig. 8. Fast carrier relaxation and recombination strongly favor the  $1X_s$  and ground-state configurations in the beginning of the evolution, but the  $2X_{sp}$ -biexciton configuration is also generated. The latter is, however, detuned from the cavity mode due to the Coulomb interaction, which leads to a strong suppression of the  $2X_{sp} \rightarrow 1X_p$  emission channel. As a consequence, excitations remain ‘trapped’ in the biexciton

configuration after the recombination from the exciton-to-ground-state emission channel has come to an end. Other recombination channels, like leaky modes, could cause a depletion of the biexciton configuration. This is demonstrated in the top left panel (dotted line), where an additional Lindblad term has been added that describes nonradiative carrier losses from the  $s$  shell at a rate of  $1/\text{ns}$ .

Uncorrelated excitation allows for a much larger number of optically inactive configurations, in which excitations are “trapped” and do not contribute to the photon production (labeled as “rest” in Fig. 8). From the realization probabilities shown in the middle row, we can infer that the formation probability of a biexciton is reduced in case of uncorrelated excitation in favor of additional configurations that cannot form in case of pairwise excitation, like the charged exciton

configurations, or configurations containing one or three electrons in arbitrary single-particle states.

The two different excitation methods do not only generate different configurations, but also have a strong impact on the interband carrier correlations. Their real parts are shown in the bottom row of Fig. 8 and yield indirect information about the prominence of various configurations. Consider for instance the interband correlation function  $C_{ssss}^x$ , which can be written as

$$C_{ssss}^x = f_s^c f_s^v - \langle c_s^\dagger c_s v_s^\dagger v_s \rangle. \quad (38)$$

Both contributions on the right-hand side can take on values between zero and one, so that  $C_{ssss}^x \in [-1, 1]$ . Its positivity is an indicator for the prominence of configurations, allowing for an optical recombination process at the  $s$  shell. This can be understood the following way: An evaluation of the configuration average  $\langle \cdot \rangle$  of the correlated part  $\langle c_s^\dagger c_s v_s^\dagger v_s \rangle$  yields a contribution for all configurations that contain an electron both in the conduction- and valence-band  $s$  states. Due to the blocked lower level these configurations do not allow for an optical recombination process. In the calculation of the factorized part  $f_s^c f_s^v$ , on the other hand, the configuration average is performed separately, so that for  $f_s^c$  ( $f_s^v$ ) all configurations contribute that contain an electron in the conduction-(valence-)band  $s$  shell, irrespective of the occupation of the valence-(conduction-)band  $s$  shell. The magnitude of both contributions in Eq. (38) depends on the relative realization probabilities of the configurations with electrons in the QD  $s$  states. An overall positive value implies  $f_s^c f_s^v > \langle c_s^\dagger c_s v_s^\dagger v_s \rangle$ , in which case the realization probabilities of the  $1X_s$  and  $2X_{sp}$  configurations exceed those of the dark  $0X_s$  configuration. Coming back to the two different excitation mechanisms, the larger number of possible configurations that contain two carriers in the two  $s$  states causes a greater weight of the correlated contribution, leading in total to a negative correlation  $C_{ssss}^x$ , as can be seen in the bottom right picture in Fig. 8. A similar argument is valid for the  $C_{spsp}^x$  contribution, which is shown together with the other possible index combinations of  $C_{ijkl}^x$  for completeness.

In this discussion, a particular point must be kept in mind: the presence of a cavity singles out a particular transition of the QD. If emission into free space is considered, contributions from charged and multiexciton configurations appear with equal likelihood, which enables a much greater variety of intraband scattering processes. The associated mode continuum prevents a solution of the vNL equation and might justify and extension of the FSH set of equations to include correlation functions with up to eight carrier operators.

### VIII. CONCLUSION

In this paper, we have presented a new approach to the treatment of electronic correlations in a nanostructure coupled to continuous electronic states, phonons, and photons. For such a system, the direct solution of the von Neumann-Lindblad (vNL) equation is only possible if the electronic Hilbert space is small, which is the case for a single or few emitters. On the other hand, Heisenberg's equation-of-motion approach, in connection with the cluster expansion method to truncate the infinite hierarchy of equations, has been used in the past as a

valuable method to describe luminescence-related phenomena, laser emission, and photon correlations for systems with many quantum dots or other active materials with a continuous density of states. In the current work, we have addressed the situation in finite-sized systems in which the small number of electronic degrees of freedom play an important role. This is, for example, the case in QDs with few confined states. We have demonstrated that boundary conditions play an important role and lead to an enhancement of correlations. For this, we have devised a formalism that combines the exact representation of the electronic degrees of freedom of the vNL approach, with the truncation of the photonic hierarchy from the cluster expansion method, resulting in the FSH ("finite-size hierarchy") method.

The second major point addressed in our work is the inclusion of scattering and dephasing by using the Lindblad formalism in the equation-of-motion-based approaches. This regards scattering and dephasing in a consistent manner and on equal footing with the Hamiltonian contributions to the time evolution of the system. A correct treatment of dissipative processes is a key requirement for making quantitative predictions in correlated systems. In earlier attempts, simpler models for the dephasing have been used to obtain an estimate for the impact of correlations, such as adding an estimated constant dephasing term to the equations of motion. Such an approach is subject to artifacts that are overcome by the presented theory.

The FSH method allows for a description of much larger systems than it is possible by means of the vNL equation, such as QD ensembles or the emission into free space via a mode continuum. For a single QD, we have presented free-space emission spectra comprising multiexcitonic effects, as well as time-resolved photoluminescence for a QD coupled to a microcavity mode. The latter case allows for a comparison with the vNL equation to benchmark the theory. The outcome is that the FSH method provides an accurate description of the dynamics predicted by the vNL equation.

### ACKNOWLEDGMENTS

We would like to thank P. Gartner for useful discussions and gratefully acknowledge financial support from the DFG research group "Quantum optics in semiconductors" and funding via the Federal Ministry of Education and Research (BMBF 01BQ1037, QK\_QuaHL-Rep).

### APPENDIX A: HAMILTONIAN

The microscopic Hamiltonian that describes the carrier dynamics and the quantized electromagnetic field contains the following contributions:

$$\mathcal{H} = \mathcal{H}_{\text{carr}}^0 + \mathcal{H}_{\text{ph}}^0 + \mathcal{H}_{\text{LM}} + \mathcal{H}_{\text{Coul}}. \quad (A1)$$

The first part of the Hamiltonian includes the noninteracting single-particle spectrum  $\varepsilon_i^{c/v}$  of the conduction- and valence-band carriers:

$$\mathcal{H}_{\text{carr}}^0 = \sum_i \varepsilon_i^c c_i^\dagger c_i + \sum_i \varepsilon_i^v v_i^\dagger v_i, \quad (A2)$$

which are annihilated (created) by the fermionic operator  $c_i$  ( $c_i^\dagger$ ) and  $v_i$  ( $v_i^\dagger$ ), respectively. Carrier-carrier interaction arises



from the two-particle Coulomb Hamiltonian

$$\begin{aligned} \mathcal{H}_{\text{Coul}} = & \frac{1}{2} \sum_{ijkl} V_{ijkl} c_i^\dagger c_j^\dagger c_k c_l \\ & + \frac{1}{2} \sum_{ijkl} V_{ijkl} v_i^\dagger v_j^\dagger v_k v_l + \sum_{ijkl} V_{ijkl} c_i^\dagger v_j^\dagger v_k c_l \\ & + \frac{1}{2} \sum_{ijkl} V_{ijkl} (v_i^\dagger v_k \delta_{jl} + v_j^\dagger v_l \delta_{ik} - v_i^\dagger v_l \delta_{jk} - v_j^\dagger v_k \delta_{il}) \\ & - \sum_{ijkl} V_{ijkl} c_i^\dagger c_l \delta_{jk}, \end{aligned} \quad (\text{A3})$$

that contains direct (Hartree) terms  $V_{ijji}$  and exchange (Fock) terms  $V_{ijij}$ , resulting in energy renormalizations and a mixing between single-particle configurations. The last two lines ensure that the contribution of the full valence band, which is already included in the single particle properties, is not double counted. The explicit form of the single-particle states enters the calculation of the Coulomb-matrix elements  $V_{ijkl}$  and is discussed in Refs. 15 and 61 for a cylindrical, lens-shaped QD. Throughout the paper we consider the single-particle wave functions in envelope-function approximation<sup>62</sup> as well as equal envelopes for the conduction- and valence-band electrons. However, more sophisticated methods, like tight-binding calculations,<sup>63</sup> can be used. For the material parameters, we have chosen those of Ref. 64 for an InGaAs/GaAs QD.

We consider the fully quantized electromagnetic field of which the free part is given by

$$\mathcal{H}_{\text{ph}}^0 = \sum_{\xi} \omega_{\xi} \left( b_{\xi}^\dagger b_{\xi} + \frac{1}{2} \right). \quad (\text{A4})$$

Here, the bosonic operators  $b_{\xi}$  ( $b_{\xi}^\dagger$ ) annihilate (create) a photon with the energy  $\omega_{\xi}$  in the photon mode  $\xi$ . The index  $\xi$  represents both, the wave vector  $\mathbf{q}$  and the polarization vector of the electromagnetic field  $\mathbf{e}_{\pm}(\mathbf{q})$ . The nonperturbative light-matter interaction  $H_{\text{LM}}$  in dipole and rotating-wave approximation reads<sup>11,15</sup>

$$\mathcal{H}_{\text{LM}} = -i \sum_{\xi,i} (g_{\xi} b_{\xi} c_i^\dagger v_i - g_{\xi}^* b_{\xi}^\dagger v_i^\dagger c_i), \quad (\text{A5})$$

where the light-matter coupling strength  $g_{\xi}$  is proportional to the interband dipole matrix element  $\mathbf{d}_{\text{cv}}$ . Note that within the envelope-function approximation, optical transitions occur only between  $s$  or the  $p$  shell of the conduction and valence bands.

In the case when the QD is resonant with a single cavity mode, the influence of all other modes can be treated via Lindblad terms, so that  $\mathcal{H}_{\text{LM}}$  reduces to the Jaynes-Cummings (JC) interaction Hamiltonian.<sup>65</sup>

## APPENDIX B: EQUATIONS OF MOTION

In this Appendix, we provide a detailed account of all contributions to the equations of motion up to the  $M_{\text{trunc}} = 1$ ,  $N_{\text{max}} = 2$  level of the FSH method that were omitted for the sake of transparency in Sec. IV. This includes contributions from the light-matter, Coulomb and system-bath interactions, which has been used for calculations shown in Secs. V and VI.

To derive the equations, we follow the same line as presented in Sec. IV. Especially the Coulomb contributions add significant complexity to the equations, thus we have checked them by utilizing the symbolic manipulation system FORM.<sup>52</sup>

### 1. Light-matter interaction

Writing down the contribution of the light-matter interaction to the equations of motion for the populations, we obtain

$$\left. \frac{d}{dt} f_i^c \right|_{\mathcal{H}_{\text{LM}}} = - \left. \frac{d}{dt} f_i^v \right|_{\mathcal{H}_{\text{LM}}} = -2\text{Re} \sum_{\xi} g_{\xi}^* \Pi_{\xi,i}, \quad (\text{B1})$$

which is coupled to the photon-assisted polarization  $\Pi_{\xi,i}$ . The corresponding dynamical equations read

$$\left. \frac{d}{dt} \Pi_{\xi,i} \right|_{\mathcal{H}_{\text{LM}}} = g_{\xi} f_i^c (1 - f_i^v) + \sum_{\mu} g_{\xi} C_{\mu ii \mu}^x \quad (\text{B2})$$

and contain the interband carrier correlation functions  $C_{ijkl}^x$ . In contrast to Eq. (17), the photon population  $\mathcal{N}_{\xi}$  and carrier-photon correlations  $\mathcal{N}_{\xi,i}^c$  and  $\mathcal{N}_{\xi,i}^v$  have been omitted as the maximum order with respect to the photons is restricted to the  $M_{\text{trunc}} = 1$  level in this Appendix.

The equations of motion for the interband carrier correlation functions,

$$\begin{aligned} \left. \frac{d}{dt} C_{ijkl}^x \right|_{\mathcal{H}_{\text{LM}}} &= \sum_{\xi} [g_{\xi} (f_j^c - f_j^v) \Pi_{\xi,i}^* + g_{\xi}^* (f_i^c - f_i^v) \Pi_{\xi,j}] \delta_{il} \delta_{jk} \\ &+ \sum_{\xi} (g_{\xi} \Pi_{\xi,ijkl}^{c*} + g_{\xi}^* \Pi_{\xi,ijkl}^c) \\ &- g_{\xi} \Pi_{\xi,ijkl}^{v*} - g_{\xi}^* \Pi_{\xi,ijkl}^v, \end{aligned} \quad (\text{B3})$$

and for the conduction band carrier-carrier correlations,

$$\begin{aligned} \left. \frac{d}{dt} C_{ijkl}^c \right|_{\mathcal{H}_{\text{LM}}} &= \sum_{\xi} (g_{\xi} \Pi_{\xi,ijlk}^{c*} - g_{\xi} \Pi_{\xi,ijkl}^{c*} \\ &+ g_{\xi}^* \Pi_{\xi,jikl}^c - g_{\xi}^* \Pi_{\xi,ijkl}^c), \end{aligned} \quad (\text{B4})$$

contain the higher-order contributions  $\Pi_{\xi,ijkl}^c$  and  $\Pi_{\xi,ijkl}^v$ , which obey their own dynamics. A similar expression can be found for the valence-band carrier-carrier correlations  $C_{ijkl}^v$  by exploiting the symmetry properties of the Hamiltonian.

Due to the limited number of considered single-particle states (see the beginning of Sec. IV), in conjunction with scattering processes that conserve the total number of excitations in the electronic system, the electronic hierarchy automatically truncates at the  $N_{\text{max}} = 2$  level. Therefore by including the equations of motion for  $\Pi_{\xi,ijkl}^c$  and  $\Pi_{\xi,ijkl}^v$ ,

$$\begin{aligned} \left. \frac{d}{dt} \Pi_{\xi,ijkl}^c \right|_{\mathcal{H}_{\text{LM}}} &= g_{\xi} C_{ijkl}^c + \left( g_{\xi}^* \Pi_{\xi,i} \Pi_{\xi,j} - g_{\xi} f_i^c f_j^c f_j^v \right. \\ &\left. + f_i^c \sum_{\mu} g_{\xi} C_{\mu j j \mu}^x \right) (\delta_{ik} \delta_{jl} - \delta_{il} \delta_{jk}) \end{aligned} \quad (\text{B5})$$

and

$$\begin{aligned} \frac{d}{dt} \Pi_{\xi,ijkl}^v \Big|_{\mathcal{H}_{LM}} &= g_{\xi} C_{ijkl}^x - g_{\xi} C_{jikl}^x \\ &+ \left( g_{\xi}^* \Pi_{\xi,l} \Pi_{\xi,k} + g_{\xi} f_k^c f_l^v f_l^v \right. \\ &\left. - f_l^v \sum_{\mu} g_{\xi} C_{\mu k k \mu}^x \right) (\delta_{il} \delta_{jk} - \delta_{ik} \delta_{jl}), \quad (\text{B6}) \end{aligned}$$

we obtain a closed set of equations at the  $M_{\text{trunc}} = 1$ ,  $N_{\text{max}} = 2$  level by neglecting the contributions from the correlation functions  $\delta \langle b_{\xi}^{\dagger} b_{\xi} c_i^{\dagger} c_j^{\dagger} c_k c_l \rangle$ ,  $\delta \langle b_{\xi}^{\dagger} b_{\xi} v_i^{\dagger} v_j^{\dagger} v_k v_l \rangle$ ,  $\delta \langle b_{\xi}^{\dagger} b_{\xi} c_i^{\dagger} v_j^{\dagger} c_k v_l \rangle$  and  $\delta \langle b_{\xi}^{\dagger} b_{\xi} v_i^{\dagger} v_j^{\dagger} c_k c_l \rangle$ , which are second order in the photon hierarchy.

At this point, we have written down equations for all occurring correlation functions. Coulomb and Lindblad contributions are discussed subsequently and only add to the quantities we have introduced.

## 2. Coulomb interaction

The inclusion of the Coulomb interaction is of central importance for the physical behavior of semiconductor nanostructures. In contrast to atomic systems, here Coulomb effects can be of similar magnitude as the energetic separation between the localized electronic states. Thus energetic shifts introduced by the Coulomb interaction can have a severe impact on dynamical and spectral properties in a system of contributing multiexciton configurations.

Starting with the contributions of the Coulomb Hamiltonian (A3) to the equations of motion for the carrier populations, we obtain

$$\frac{d}{dt} f_i^c \Big|_{\mathcal{H}_{\text{Coul}}} = -2\text{Im} \sum_{\mu\nu\alpha} V_{i\mu\nu\alpha} C_{i\mu\alpha\nu}^{x+c}. \quad (\text{B7})$$

Here, we have introduced the abbreviation  $C_{ijkl}^{x+c} = C_{ijkl}^x + C_{ijkl}^c$ . For the higher-order correlation functions, a straightforward interpretation of the contributions is obscured by their complexity, and we restrain ourselves to a mere listing of equations:

$$\begin{aligned} \frac{d}{dt} \Pi_{\xi,i} \Big|_{\mathcal{H}_{\text{Coul}}} &= i \sum_{\mu} \left\{ V_{i\mu i \mu} [(1 + f_{\mu}^c - f_{\mu}^v) \Pi_{\xi,i} - (f_i^c - f_i^v) \Pi_{\xi,\mu}] + \sum_{\nu\alpha} V_{i\mu\nu\alpha} (\Pi_{\xi,\mu i \nu\alpha}^c + \Pi_{\xi,i\mu\alpha\nu}^v) \right. \\ &\left. + \sum_{\nu\alpha} V_{i\mu\nu\alpha}^* (\Pi_{\xi,\nu\alpha i \mu}^c + \Pi_{\xi,\nu\alpha i \mu}^v) \right\}, \quad (\text{B8}) \end{aligned}$$

$$\begin{aligned} \frac{d}{dt} C_{ijkl}^x \Big|_{\mathcal{H}_{\text{Coul}}} &= i V_{ijkl}^* (f_i^c f_j^v - f_k^c f_l^v) + i \sum_{\mu\nu} [V_{ij\mu\nu}^* C_{\nu\mu k l}^x - V_{kl\mu\nu} C_{ij\nu\mu}^x + V_{k\mu\nu} C_{ij\nu l}^x - V_{i\mu\nu}^* C_{\nu j k l}^x] \\ &+ i \sum_{\mu\nu} [(V_{l\mu\nu} - V_{l\nu\mu}) C_{ij k \nu}^x + (V_{j\mu\nu}^* - V_{j\nu\mu}^*) C_{i\nu k l}^x] - i \sum_{\mu} [V_{i\mu\mu k}^* (f_i^c - f_k^c) f_j^v \delta_{j l} \\ &+ (V_{j\mu l}^* - V_{j\mu l}^*) f_i^c (f_l^v - f_j^v) \delta_{i k}] - 2\text{Im} \left\{ \sum_{\mu\nu\alpha} [f_j^v V_{i\mu\nu\alpha} C_{i\mu\alpha\nu}^{x+c} + f_i^c V_{j\mu\nu\alpha} C_{\mu j \nu\alpha}^{x+v}] \right\} \delta_{i k} \delta_{j l}, \quad (\text{B9}) \end{aligned}$$

$$\begin{aligned} \frac{d}{dt} C_{ijkl}^c \Big|_{\mathcal{H}_{\text{Coul}}} &= i (V_{ijkl}^* - V_{ijlk}^*) (f_k^c f_l^c - f_i^c f_j^c) + i \sum_{\mu\nu} [V_{l\mu\nu} C_{ij k \nu}^c - V_{k\mu\nu} C_{ij l \nu}^c + V_{kl\mu\nu} C_{ij \mu\nu}^c \\ &+ V_{i\mu\nu}^* C_{j\nu k l}^c - V_{j\mu\nu}^* C_{i\nu k l}^c - V_{ij\mu\nu}^* C_{\mu\nu k l}^c] + i \sum_{\mu} [V_{i\mu\mu k}^* f_j^c (f_k^c - f_i^c) \delta_{j l} - V_{i\mu\mu l}^* f_j^c (f_l^c - f_i^c) \delta_{j k}] \\ &- i \sum_{\mu} [V_{j\mu\mu k}^* f_i^c (f_k^c - f_j^c) \delta_{i l} - V_{j\mu\mu l}^* f_i^c (f_l^c - f_j^c) \delta_{i k}] - 2\text{Im} \left\{ \sum_{\mu\nu\alpha} [f_j^c (V_{i\mu\nu\alpha} C_{i\mu\alpha\nu}^{x+c}) \right. \\ &\left. + f_i^c (V_{j\mu\nu\alpha} C_{j\mu\alpha\nu}^{x+c}) \right\} (\delta_{i k} \delta_{j l} - \delta_{i l} \delta_{j k}), \quad (\text{B10}) \end{aligned}$$

$$\begin{aligned} \frac{d}{dt} \Pi_{\xi,ijkl}^c \Big|_{\mathcal{H}_{\text{Coul}}} &= i \sum_{\mu\nu} [V_{l\mu\nu} \Pi_{\xi,ij k \nu}^c - V_{k\mu\nu} \Pi_{\xi,ij l \nu}^c + V_{kl\mu\nu} \Pi_{\xi,ij \mu\nu}^c - V_{i\mu\nu}^* \Pi_{\xi,\nu j k l}^c + V_{ij\mu\nu}^* \Pi_{\xi,\nu\mu k l}^c \\ &+ (V_{j\mu\nu}^* - V_{j\mu\nu}^*) \Pi_{\xi,i\nu k l}^c] + i [V_{ijkl}^* (f_l^c \Pi_{\xi,k} - f_i^c \Pi_{\xi,j}) - V_{ijlk}^* (f_k^c \Pi_{\xi,l} - f_i^c \Pi_{\xi,j})] \\ &+ i f_i^c \sum_{\mu} \{ [V_{j\mu\mu k}^* (\Pi_{\xi,j} - \Pi_{\xi,k}) + V_{j\mu k \mu}^* \Pi_{\xi,k}] \delta_{i l} - [V_{j\mu\mu l}^* (\Pi_{\xi,j} - \Pi_{\xi,l}) + V_{j\mu l \mu}^* \Pi_{\xi,l}] \delta_{i k} \} \\ &+ i \Pi_{\xi,j} \sum_{\mu} [V_{i\mu\mu k}^* (f_k^c - f_i^c) \delta_{j l} - V_{i\mu\mu l}^* (f_l^c - f_i^c) \delta_{j k}] - 2\Pi_{\xi,j} \text{Im} \left( \sum_{\mu\nu\alpha} V_{i\mu\nu\alpha} C_{i\mu\alpha\nu}^{x+c} \right) (\delta_{i k} \delta_{j l} - \delta_{i l} \delta_{j k}) \\ &+ i f_i^c \sum_{\mu\nu\alpha} [V_{j\mu\nu\alpha} (\Pi_{\xi,\mu j \nu\alpha}^c + \Pi_{\xi,j\mu\alpha\nu}^v) + V_{j\mu\nu\alpha}^* (\Pi_{\xi,\nu\alpha j \mu}^c + \Pi_{\xi,\nu\alpha j \mu}^v)] (\delta_{i k} \delta_{j l} - \delta_{i l} \delta_{j k}) \\ &+ i f_i^c \sum_{\mu} V_{j\mu j \mu} [ \Pi_{\xi,j} (1 - f_{\mu}^v + f_{\mu}^c) - \Pi_{\xi,\mu} (f_j^c - f_j^v) ] (\delta_{i k} \delta_{j l} - \delta_{i l} \delta_{j k}), \quad (\text{B11}) \end{aligned}$$

$$\begin{aligned}
\left. \frac{d}{dt} \Pi_{\xi,ijkl}^v \right|_{\mathcal{H}_{\text{Coul}}} &= -i V_{ijkl}^* (\Pi_{\xi,j} f_i^v - \Pi_{\xi,k} f_l^v) + i V_{ijlk}^* (\Pi_{\xi,i} f_j^v - \Pi_{\xi,k} f_l^v) - i \sum_{\mu} \{ V_{k\mu k\mu} [\Pi_{\xi,\mu} (f_k^c - f_k^v) \\
&\quad - \Pi_{\xi,k} (f_{\mu}^c + f_{\mu}^h)] \} f_l^v (\delta_{ik} \delta_{jl} - \delta_{il} \delta_{jk}) + i \sum_{\mu\nu\alpha} [V_{k\mu\nu\alpha} (\Pi_{\xi,\mu k\nu\alpha}^c + \Pi_{\xi,k\mu\alpha\nu}^v) \\
&\quad + V_{k\mu\nu\alpha}^* (\Pi_{\xi,\nu\alpha k\mu}^c + \Pi_{\xi,\nu\alpha k\mu}^v)] f_l^v (\delta_{ik} \delta_{jl} - \delta_{il} \delta_{jk}) - 2\Pi_{\xi,k} \text{Im} \left( \sum_{\mu\nu\alpha} V_{l\mu\nu\alpha} C_{\mu l\nu\alpha}^{x+v} \right) (\delta_{ik} \delta_{jl} - \delta_{il} \delta_{jk}) \\
&\quad + i \sum_{\mu\nu} [V_{k\mu\nu} \Pi_{\xi,ij\nu l}^v - V_{kl\mu\nu} \Pi_{\xi,ij\nu\mu}^v + (V_{l\mu\nu} - V_{l\nu\mu}) \Pi_{\xi,ijk\nu}^v] \\
&\quad + i \sum_{\mu\nu} [(V_{i\mu\nu}^* - V_{i\nu\mu}^*) \Pi_{\xi,j\nu kl}^v - V_{ij\mu\nu}^* \Pi_{\xi,\mu\nu kl}^v + (V_{j\mu\nu}^* - V_{j\nu\mu}^*) \Pi_{\xi,i\nu kl}^v] \\
&\quad - i \Pi_{\xi,k} \sum_{\mu} [(V_{i\mu k\mu}^* - V_{i\mu k\mu}^*) \delta_{jl} - (V_{j\mu k\mu}^* - V_{j\mu k\mu}^*) \delta_{il}] f_l^v - i \Pi_{\xi,k} \sum_{\mu} [(V_{i\mu l\mu}^* - V_{i\mu l\mu}^*) (f_i^v - f_l^v) \delta_{jk} \\
&\quad - (V_{j\mu l\mu}^* - V_{j\mu l\mu}^*) (f_j^v - f_l^v) \delta_{ik}] - i f_l^v \sum_{\mu} [V_{i\mu\mu k}^* \Pi_{\xi,i} \delta_{jl} - V_{j\mu\mu k}^* \Pi_{\xi,j} \delta_{il}]. \tag{B12}
\end{aligned}$$

### 3. System-bath interaction

The evaluation of the system-bath contributions follows from Eq. (14). Cavity losses have already been included in the discussion in Sec. IV.

#### a. Scattering

The physical effects of the intraband scattering processes listed in the following include carrier redistribution, dephasing, and redistribution of correlation strength in compliance with the sum rule (27) as well as effects on higher-order correlation functions. Note that the evaluation of the sum for  $\mu \neq \nu$  in Eq. (23) formally requires setting  $\gamma_{\mu\mu}^{cc} = 0$ .

$$\left. \frac{d}{dt} f_i^c \right|_{\text{scatt}} = \sum_{\mu} \gamma_{i\mu}^{cc} [f_{\mu}^c (1 - f_i^c) + C_{i\mu i\mu}^c] - \sum_{\mu} \gamma_{\mu i}^{cc} [f_i^c (1 - f_{\mu}^c) + C_{i\mu i\mu}^c], \tag{B13}$$

$$\left. \frac{d}{dt} \Pi_{\xi,i} \right|_{\text{scatt}} = -\frac{1}{2} \sum_{\mu} \gamma_{\mu i}^{cc} \Pi_{\xi,i} + \frac{1}{2} \sum_{\mu} (\gamma_{\mu i}^{cc} - \gamma_{i\mu}^{cc}) (f_{\mu}^c \Pi_{\xi,i} + \Pi_{\xi,\mu i i\mu}^c), \tag{B14}$$

$$\left. \frac{d}{dt} C_{ijkl}^x \right|_{\text{scatt}} = \sum_{\mu} \left[ \gamma_{i\mu}^{cc} C_{\mu j l\mu}^x \delta_{ik} - \frac{1}{2} (\gamma_{\mu i}^{cc} + \gamma_{\mu k}^{cc}) C_{ijkl}^x \right] - \sum_{\mu} (\gamma_{i\mu}^{cc} - \gamma_{\mu i}^{cc}) (f_i^c f_{\mu}^c - C_{i\mu i\mu}^c) f_j^v \delta_{ik} \delta_{jl}, \tag{B15}$$

$$\begin{aligned}
\left. \frac{d}{dt} C_{ijkl}^c \right|_{\text{scatt}} &= \frac{1}{2} (\gamma_{ij}^{cc} + \gamma_{ji}^{cc} + \gamma_{kl}^{cc} + \gamma_{lk}^{cc}) C_{ijkl}^c + [\gamma_{ij}^{cc} f_j^c (f_j^c - f_i^c) - \gamma_{ji}^{cc} f_i^c (f_j^c - f_i^c)] (\delta_{ik} \delta_{jl} - \delta_{il} \delta_{jk}) \\
&\quad - \frac{1}{2} \sum_{\mu} (\gamma_{\mu i}^{cc} + \gamma_{\mu j}^{cc} + \gamma_{\mu k}^{cc} + \gamma_{\mu l}^{cc}) C_{ijkl}^c + \sum_{\mu} (\gamma_{\mu i}^{cc} - \gamma_{i\mu}^{cc} + \gamma_{\mu j}^{cc} - \gamma_{j\mu}^{cc}) f_i^c f_j^c f_{\mu}^c (\delta_{ik} \delta_{jl} - \delta_{il} \delta_{jk}) \\
&\quad + \sum_{\mu} \gamma_{i\mu}^{cc} (C_{j\mu l\mu}^c \delta_{ik} - C_{j\mu k\mu}^c \delta_{il}) + \sum_{\mu} \gamma_{j\mu}^{cc} (C_{i\mu k\mu}^c \delta_{jl} - C_{i\mu l\mu}^c \delta_{jk}) + \sum_{\mu} [(\gamma_{i\mu}^{cc} - \gamma_{\mu i}^{cc}) f_j^c C_{i\mu i\mu}^c \\
&\quad + (\gamma_{j\mu}^{cc} - \gamma_{\mu j}^{cc}) f_i^c C_{j\mu j\mu}^c] (\delta_{ik} \delta_{jl} - \delta_{il} \delta_{jk}), \tag{B16}
\end{aligned}$$

$$\begin{aligned}
\left. \frac{d}{dt} \Pi_{\xi,ijkl}^c \right|_{\text{scatt}} &= \frac{1}{2} (\gamma_{kl}^{cc} + \gamma_{lk}^{cc}) \Pi_{\xi,ijkl}^c + \left[ \gamma_{ij}^{cc} \left( f_j^c - \frac{1}{2} f_i^c \right) - \frac{1}{2} \gamma_{ji}^{cc} f_i^c \right] \Pi_{\xi,j} (\delta_{ik} \delta_{jl} - \delta_{il} \delta_{jk}) \\
&\quad - \frac{1}{2} \sum_{\mu} (\gamma_{\mu i}^{cc} + \gamma_{\mu k}^{cc} + \gamma_{\mu l}^{cc}) \Pi_{\xi,ijkl}^c + \sum_{\mu} \gamma_{i\mu}^{cc} (\Pi_{\xi,\mu j k\mu}^c \delta_{il} - \Pi_{\xi,\mu j l\mu}^c \delta_{ik}) \\
&\quad + \sum_{\mu} \left[ (\gamma_{\mu i}^{cc} - \gamma_{i\mu}^{cc}) (f_i^c f_{\mu}^c - C_{i\mu i\mu}^c) \Pi_{\xi,j} + \frac{1}{2} (\gamma_{\mu j}^{cc} - \gamma_{j\mu}^{cc}) (f_{\mu}^c \Pi_{\xi,j} + \Pi_{\xi,\mu j j\mu}^c) f_i^c \right] (\delta_{ik} \delta_{jl} - \delta_{il} \delta_{jk}), \tag{B17}
\end{aligned}$$

$$\left. \frac{d}{dt} \Pi_{\xi,ijkl}^v \right|_{\text{scatt}} = -\frac{1}{2} \sum_{\mu} \gamma_{\mu k}^{cc} \Pi_{\xi,ijkl}^v - \frac{1}{2} \sum_{\mu} (\gamma_{k\mu}^{cc} - \gamma_{\mu k}^{cc}) f_l^v (f_{\mu}^c \Pi_{\xi,k} + \Pi_{\xi,\mu k k\mu}^c) (\delta_{ik} \delta_{jl} - \delta_{il} \delta_{jk}). \tag{B18}$$

A similar set of equations can be given for the intraband scattering in the valence band.

### b. Pumping

In Eq. (28), we have formulated the Lindblad contribution for pairwise carrier capture into the QD  $p$  states. For a general capture into the state  $|\mu\rangle$  at a rate  $P_\mu(t)$ , this equation reads

$$\left. \frac{d}{dt} \langle A \rangle \right|_{\text{pump}} = \frac{P_\mu(t)}{2} (\langle [v_\mu^\dagger c_\mu, A] c_\mu^\dagger v_\mu \rangle + \langle v_\mu^\dagger c_\mu [A, c_\mu^\dagger v_\mu] \rangle) \quad (\text{B19})$$

and leads to the following contributions in the set of equations of motion:

$$\left. \frac{d}{dt} f_i^c \right|_{\text{pump}} = P_i(t) [(1 - f_i^c) f_i^v + C_{iii}^x], \quad (\text{B20})$$

$$\left. \frac{d}{dt} \Pi_{\xi,i} \right|_{\text{pump}} = -\frac{1}{2} P_i(t) \Pi_{\xi,i}, \quad (\text{B21})$$

$$\begin{aligned} \left. \frac{d}{dt} C_{ijkl}^x \right|_{\text{pump}} &= -\frac{1}{2} [P_j(t) + P_l(t)] C_{ijkl}^x + P_i(t) C_{ijil}^v \delta_{ik} + \frac{1}{2} [P_i(t) C_{ikil}^x \delta_{ij} + P_k(t) C_{ijkk}^x \delta_{kl}] \\ &\quad + P_i(t) (C_{iii}^x - f_i^c f_i^v) f_j^v \delta_{ik} \delta_{jl} + P_j(t) (f_i^c f_j^v - C_{jjj}^x) f_i^c \delta_{ik} \delta_{jl} + P_i(t) (f_i^v f_i^c - f_i^c f_i^v) \delta_{ij} \delta_{ik} \delta_{il}, \end{aligned} \quad (\text{B22})$$

$$\begin{aligned} \left. \frac{d}{dt} C_{ijkl}^c \right|_{\text{pump}} &= +P_i(t) (C_{jili}^x \delta_{ik} - C_{jiki}^x \delta_{il}) + P_j(t) (C_{ijjk}^x \delta_{jl} - C_{ijlj}^x \delta_{jk}) \\ &\quad + P_i(t) f_j^c (C_{iii}^x - f_i^v f_i^c) (\delta_{ik} \delta_{jl} - \delta_{il} \delta_{jk}) + P_j(t) f_i^c (C_{jjj}^x - f_j^v f_j^c) (\delta_{ik} \delta_{jl} - \delta_{il} \delta_{jk}), \end{aligned} \quad (\text{B23})$$

$$\left. \frac{d}{dt} \Pi_{\xi,ijkl}^c \right|_{\text{pump}} = -\frac{1}{2} P_j(t) \Pi_{\xi,ijkl}^c + \frac{1}{2} P_i(t) (\Pi_{\xi,iiik}^c \delta_{ij} + 2\Pi_{\xi,ijki}^v \delta_{il} - 2\Pi_{\xi,ijli}^v \delta_{ik}) + P_i(t) \Pi_{\xi,j} (C_{iii}^x - f_i^v f_i^c) (\delta_{ik} \delta_{jl} - \delta_{il} \delta_{jk}), \quad (\text{B24})$$

$$\left. \frac{d}{dt} \Pi_{\xi,ijkl}^v \right|_{\text{pump}} = -\frac{1}{2} [P_i(t) + P_j(t) + P_l(t)] \Pi_{\xi,ijkl}^v + \frac{1}{2} P_k(t) \Pi_{\xi,ijkk}^v \delta_{kl} + P_l(t) \Pi_{\xi,k} (f_l^v f_l^c - C_{lll}^x) (\delta_{ik} \delta_{jl} - \delta_{il} \delta_{jk}). \quad (\text{B25})$$

<sup>1</sup>Z. I. Alferov, *Rev. Mod. Phys.* **73**, 767 (2001).

<sup>2</sup>D. Bimberg, M. Grundmann, and N. N. Ledentsov, *Quantum Dot Heterostructures*, 1st ed. (John Wiley and Sons, Chichester, UK, 1998).

<sup>3</sup>S. Strauf and F. Jahnke, *Laser Photon. Rev.* **5**, 607 (2011).

<sup>4</sup>W. W. Chow, M. Lorke, and F. Jahnke, *IEEE J. Sel. Top. Quantum Electron.* **17**, 1349 (2011).

<sup>5</sup>J. Hendrickson, B. C. Richards, J. Sweet, S. Mosor, C. Christenson, D. Lam, G. Khitrova, H. M. Gibbs, T. Yoshie, A. Scherer *et al.*, *Phys. Rev. B* **72**, 193303 (2005).

<sup>6</sup>S. Strauf, K. Hennessy, M. T. Rakher, Y.-S. Choi, A. Badolato, L. C. Andreani, E. L. Hu, P. M. Petroff, and D. Bouwmeester, *Phys. Rev. Lett.* **96**, 127404 (2006).

<sup>7</sup>S. Reitzenstein, A. Bazhenov, A. Gorbunov, C. Hofmann, S. Münch, A. Löffler, M. Kamp, J. P. Reithmaier, V. D. Kulakovskii, and A. Forchel, *Appl. Phys. Lett.* **89**, 051107 (2006).

<sup>8</sup>E. Peter, P. Senellart, D. Martrou, A. Lemaitre, J. Hours, J. M. Gérard, and J. Bloch, *Phys. Rev. Lett.* **95**, 067401 (2005).

<sup>9</sup>K. Baumann and G. C. Hegerfeldt, *Publ. RIMS Kyoto Univ.* **21**, 191 (1985).

<sup>10</sup>H. Schoeller, *Ann. Phys.* **229**, 273 (1994).

<sup>11</sup>M. Kira, F. Jahnke, W. Hoyer, and S. W. Koch, *Prog. Quantum Electron.* **23**, 189 (1999).

<sup>12</sup>W. Hoyer, M. Kira, and S. W. Koch, *Phys. Rev. B* **67**, 155113 (2003).

<sup>13</sup>C. Gies, J. Wiersig, M. Lorke, and F. Jahnke, *Phys. Rev. A* **75**, 013803 (2007).

<sup>14</sup>T. Feldtmann, L. Schneebeli, M. Kira, and S. W. Koch, *Phys. Rev. B* **73**, 155319 (2006).

<sup>15</sup>N. Baer, C. Gies, J. Wiersig, and F. Jahnke, *Eur. Phys. J. B* **50**, 411 (2006).

<sup>16</sup>M. Schwab, H. Kurtze, T. Auer, T. Berstermann, M. Bayer, J. Wiersig, N. Baer, C. Gies, F. Jahnke, J. P. Reithmaier *et al.*, *Phys. Rev. B* **74**, 045323 (2006).

<sup>17</sup>T. Berstermann, T. Auer, H. Kurtze, M. Schwab, D. R. Yakovlev, M. Bayer, J. Wiersig, C. Gies, F. Jahnke, D. Reuter *et al.*, *Phys. Rev. B* **76**, 165318 (2007).

<sup>18</sup>J. Fricke, *Ann. Phys. (NY)* **252**, 479 (1996).

<sup>19</sup>S. M. Ulrich, C. Gies, S. Ates, J. Wiersig, S. Reitzenstein, C. Hofmann, A. Löffler, A. Forchel, F. Jahnke, and P. Michler, *Phys. Rev. Lett.* **98**, 043906 (2007).

<sup>20</sup>A. Krügel, V. M. Axt, and T. Kuhn, *Phys. Rev. B* **73**, 035302 (2006).

<sup>21</sup>M. Kira, F. Jahnke, and S. W. Koch, *Phys. Rev. Lett.* **81**, 3263 (1998).

<sup>22</sup>T. Kohler and K. Burnett, *Phys. Rev. A* **65**, 033601 (2002).

<sup>23</sup>M. D. Kapetanakis and I. E. Perakis, *Phys. Rev. Lett.* **101**, 097201 (2008).

<sup>24</sup>M. Richter, A. Carmele, A. Sitek, and A. Knorr, *Phys. Rev. Lett.* **103**, 087407 (2009).

<sup>25</sup>A. Carmele, M. Richter, W. W. Chow, and A. Knorr, *Phys. Rev. Lett.* **104**, 156801 (2010).

<sup>26</sup>J. Kabuss, A. Carmele, T. Brandes, and A. Knorr, *Phys. Rev. Lett.* **109**, 054301 (2012).

<sup>27</sup>M. Mootz, M. Kira, and S. W. Koch, *J. Opt. Soc. Am. B* **29**, A17 (2012).

- <sup>28</sup>M. Kira, S. W. Koch, R. P. Smith, A. E. Hunter, and S. T. Cundiff, *Nat. Phys.* **7**, 799 (2011).
- <sup>29</sup>G. J. Beirne, M. Reischle, R. Rossbach, W.-M. Schulz, M. Jetter, J. Seebeck, P. Gartner, C. Gies, F. Jahnke, and P. Michler, *Phys. Rev. B* **75**, 195302 (2007).
- <sup>30</sup>Y. Mu and C. M. Savage, *Phys. Rev. A* **46**, 5944 (1992).
- <sup>31</sup>F. Troiani, J. I. Perea, and C. Tejedor, *Phys. Rev. B* **74**, 235310 (2006).
- <sup>32</sup>E. del Valle, F. P. Laussy, and C. Tejedor, *Phys. Rev. B* **79**, 235326 (2009).
- <sup>33</sup>S. Ritter, P. Gartner, C. Gies, and F. Jahnke, *Opt. Express* **18**, 9909 (2010).
- <sup>34</sup>C. Gies, M. Florian, P. Gartner, and F. Jahnke, *Opt. Express* **19**, 14370 (2011).
- <sup>35</sup>A. Steinhoff, P. Gartner, M. Florian, and F. Jahnke, *Phys. Rev. B* **85**, 205144 (2012).
- <sup>36</sup>G. Lindblad, *Commun. Math. Phys.* **48**, 119 (1976).
- <sup>37</sup>H.-P. Breuer and F. Petruccione, *The Theory of Open Quantum Systems* (Oxford University Press, New York, USA, 2007).
- <sup>38</sup>C. Roy and S. Hughes, *Phys. Rev. X* **1**, 021009 (2011).
- <sup>39</sup>U. Hohenester, *Phys. Rev. B* **81**, 155303 (2010).
- <sup>40</sup>C. Gies, M. Florian, P. Gartner, and F. Jahnke, in *Quantum Optics With Semiconductor Nanostructures*, edited by F. Jahnke, 1st ed. (Woodhead, Cambridge, UK, 2012).
- <sup>41</sup>J. Seebeck, T. R. Nielsen, P. Gartner, and F. Jahnke, *Phys. Rev. B* **71**, 125327 (2005).
- <sup>42</sup>E. A. Zibik, L. R. Wilson, R. P. Green, G. Bastard, R. Ferreira, P. J. Phillips, D. A. Carder, J.-P. R. Wells, J. W. Cockburn, M. S. Skolnick *et al.*, *Phys. Rev. B* **70**, 161305 (2004).
- <sup>43</sup>S. Xu, A. A. Mikhailovsky, J. A. Hollingsworth, and V. I. Klimov, *Phys. Rev. B* **65**, 045319 (2002).
- <sup>44</sup>J. Urayama, T. B. Norris, J. Singh, and P. Bhattacharya, *Phys. Rev. Lett.* **86**, 4930 (2001).
- <sup>45</sup>H. J. Carmichael, *Statistical Methods in Quantum Optics 1: Master Equations and Fokker-Planck Equations (Theoretical and Mathematical Physics)* (Springer-Verlag, Berlin, Heidelberg, New York, 2003), Vol. 1.
- <sup>46</sup>M. Lorke, T. R. Nielsen, J. Seebeck, P. Gartner, and F. Jahnke, *Phys. Rev. B* **73**, 085324 (2006).
- <sup>47</sup>K. Schuh, P. Gartner, and F. Jahnke, *Phys. Rev. B* **87**, 035301 (2013).
- <sup>48</sup>P. Borri, W. Langbein, S. Schneider, U. Woggon, R. L. Sellin, D. Ouyang, and D. Bimberg, *Phys. Rev. Lett.* **87**, 157401 (2001).
- <sup>49</sup>J. Fricke, *Transportgleichungen für quantenmechanische Vielteilchensysteme* (Cuvillier Verlag, Göttingen, 1996).
- <sup>50</sup>The following discussion is strictly valid in the singlet approximation, where all carrier contributions are formulated in terms of populations. At the doublet level, additional correlations are included.
- <sup>51</sup>U. Hohenester, F. Rossi, and E. Molinari, *Solid State Commun.* **111**, 187 (1999).
- <sup>52</sup>J. A. M. Vermaseren, [arXiv:math-ph/0010025](https://arxiv.org/abs/math-ph/0010025).
- <sup>53</sup>Y. Ota, S. Iwamoto, N. Kumagai, and Y. Arakawa, *Phys. Rev. Lett.* **107**, 233602 (2011).
- <sup>54</sup>U. Bockelmann and T. Egeler, *Phys. Rev. B* **46**, 15574 (1992).
- <sup>55</sup>I. Vurgaftman, Y. Lam, and J. Singh, *Phys. Rev. B* **50**, 14309 (1994).
- <sup>56</sup>T. Inoshita and H. Sakaki, *Phys. Rev. B* **56**, 4355 (1997).
- <sup>57</sup>M. Brasken, M. Lindberg, M. Söpanen, H. Lipsanen, and J. Tulkki, *Phys. Rev. B* **58**, 15993 (1998).
- <sup>58</sup>H. Jiang and J. Singh, *IEEE J. Quantum Electron.* **34**, 1188 (1998).
- <sup>59</sup>T. Stauber, R. Zimmermann, and H. Castella, *Phys. Rev. B* **62**, 7336 (2000).
- <sup>60</sup>M. Nomura, N. Kumagai, S. Iwamoto, Y. Ota, and Y. Arakawa, *Nat. Phys.* **6**, 279 (2010).
- <sup>61</sup>A. Wojs, P. Hawrylak, S. Fafard, and L. Jacak, *Phys. Rev. B* **54**, 5604 (1996).
- <sup>62</sup>H. Haug and S. Koch, *Quantum Theory of the Optical and Electronic Properties of Semiconductors*, 4th ed. (World Scientific, Singapore, 2004).
- <sup>63</sup>S. Schulz and G. Czycholl, *Phys. Rev. B* **72**, 165317 (2005).
- <sup>64</sup>N. Baer, P. Gartner, and F. Jahnke, *Eur. Phys. J. B* **42**, 231 (2004).
- <sup>65</sup>E. Jaynes and F. Cummings, *Proc. IEEE* **51**, 89 (1963).